Dynamic Testing of GE Multilin 869 Motor Protection Relay for Stator Inter-turn Faults

by

Sallena Choudhury

to obtain the degree of Master of Science in Electrical Engineering
at the Delft University of Technology,
to be defended publicly on Monday August 30, 2021 at 09:00 AM.

Student number:	5121833	
Project duration:	November 20, 2020 – August 30, 2021	
Thesis committee:	Dr. ing. Marjan Popov,	TU Delft, Supervisor
	Dr. Alex Stefanov,	TU Delft
	Dr. Mohamad Ghaffarian Niasar,	TU Delft
	Ir. Steven de Clippelaar,	DOW Benelux

Faculty of Electrical Engineering, Mathematics and Computer Science (EEMCS)
Delft University of Technology

TU Delft Delft University of Technology

Science, for me, gives a partial explanation for life.
In so far as it goes, it is based on fact,
experience and experiment

Rosalind Franklin

Abstract

Induction motors have a significant role in every aspect of modern living. They are extensively used in every industry because of their robust construction, easy operation, controllable and adaptable features. Therefore, occurrence of faults in these machines are a major concern. The protection schemes implemented in a network plays an important role in the safe operation of the machine. The key component of common protection schemes is a relay that senses abnormalities in the network and separates the faulty section from the healthy network.

Large faults such as phase faults, phase-to-phase faults are easily detected as they impact the whole network. However, commonly occurring faults such as stator winding faults, bearing faults, etc. are difficult to detect using the standardised protection schemes. Stator winding faults create localised heating that can rapidly incite phase faults. Thus, additional protection schemes are required to detect them in time.

This thesis focuses on modelling and simulation of stator inter-turn faults in an induction motor using Electromagnetic Transient Program (EMTP)-Alternative Transients Program (ATP) platform; dynamic testing of a chosen relay at various fault severities and fault resistances. Finally, optimised settings of the chosen relay are suggested for a given medium power induction motor and the results are discussed.

Acknowledgements

This thesis was conducted in Intelligent Electric Power Grids (IEPG) group of Electrical Sustainable Energy department under the Faculty of EEMCS at TU Delft. This was a great opportunity for me to gain some valuable research experience and this would not have been possible without people who have challenged and motivated me throughout my time here.

I would first like to thank Dr. ing. Marjan Popov, my supervisor for this thesis. He has been a constant source of motivation and support through my studies, internship as well as my thesis. He has provided valuable guidance, constant encouragement and a platform for me to gain insight in this interesting field.

Secondly, I would also like to thank Ir. Steven De Clippelaar, Power System Engineer at DOW Chemical Energy Tech Center for his continuous support in all aspects of the model designing. Thank you for sharing your knowledge and experience throughout the duration of this thesis.

Thirdly, I would also like to thank Robert Muziol, Application Specialist at GE Grid Automation for his support in relay testing. Thank you for sharing your expertise in the field of relay testing.

I would also like to thank the committee members Dr. Alex Stefanov and Dr. Mohamad Ghafarrian Niasar for evaluating my thesis and taking time to be part of the thesis committee.

This experience in TU Delft has been a truly unique one, given that there was a pandemic amidst the course. I would like to really appreciate all my professors, especially the ones in the Smart AC and DC grids profile, who helped me gain deep understanding much necessary for conducting this research. All of us were forced to adapt to new circumstances, but everybody tried their hardest to make the transition really seamless, and I thank them for that.

Finally, I would like to take this opportunity to thank my parents, sister and friends. They have always supported and motivated me throughout my stay in the Netherlands. This has been a journey of fun, frustration and insight which I'm happy to have experienced with all these people around. Thank you for the memories!

Sallena Choudhury
Delft, August 2021

Contents

List of Figures

List of Tables

List of Abbreviations

ATP Alternative Transients Program

COMTRADE Common format for Transient Data Exchange

EMF Electromotive Force

EMTP Electromagnetic Transient Program

EPRI Electric Power Research Institute

MMF Magnetomotive Force

UMIND Universal Induction Machine with Manufacturer's Data Input

1

Introduction

The most widely used machine to convert electrical energy to mechanical energy is an induction motor. Due to their extensive usage in every industry, they are called the workhorses of the industry. They have a strong demand in industrial applications owing to their robust construction, reliability and safety. However, when the operation of an induction machine is interrupted abruptly, it operates under faulty conditions. These could also be caused by mechanical and electrical imperfections in the machine. Electric Power Research Institute (EPRI) conducted a survey to determine the distribution of failed components in an induction machine. In this survey, the faults were broadly categorised into four types: bearing, rotor, stator winding and others [1]. Figure 1.1 depicts the results of the survey according to which, stator winding faults account for 38% of all faults [1].

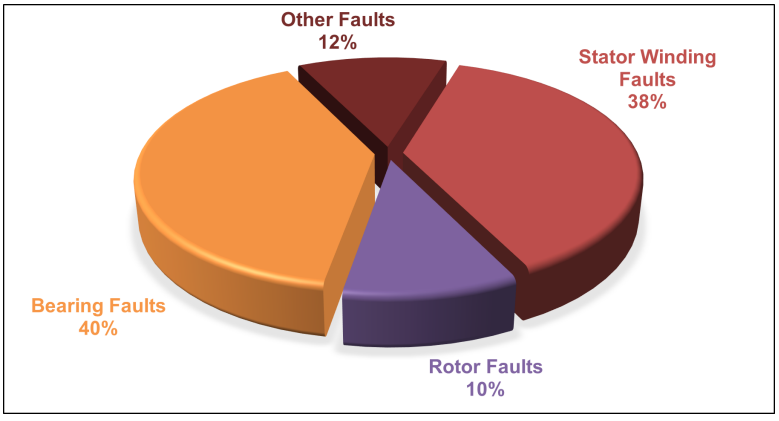

Figure 1.1: Percentage chart of faults in an induction motor [1]

1

In most cases, a stator inter-turn fault is caused by thermal stress, vibrations and ageing process during the operational phase [2]–[4]. These failures affect the industries due to the increased downtime of the process. Therefore, proper protection is required to avoid these unwanted disturbances in the process. This thesis aims at replicating a stator inter-turn fault in a given induction motor, detect and optimise the protection relay settings through dynamic testing, even at extremely low fault severity.

1.1. Problem Definition

Induction machines are expected to have high reliability and long life. This can be attained by periodic performance checks throughout the life cycle of the machine. However, frequent maintenance checks are expensive and will result in production losses. Therefore, accurate online monitoring and diagnosis of frequently occurring faults is called for. One of these frequently occurring faults is stator inter-turn fault. This fault can propagate rapidly into a phase-fault and can cause huge damage. The conventional protection schemes fail to detect this fault at an early stage. Thus, additional protection schemes are required to identify these faults in time.

1.2. Research Questions

Based on the presented problem, the following research questions are set to be answered through this thesis research.

1. How can an induction motor be modelled accurately, to detect stator inter-turn faults?
2. How can the fault current resulting from a stator inter-turn fault be detected considering its low magnitude?
3. What is the principle of stator inter-turn fault detection in the chosen protection relay?
4. What are the suitable settings in the chosen protection relay to detect stator inter-turn fault with least severity, without causing any false trips?

1.3. Thesis Scope

The flowchart presented in Figure 1.2 describes the procedure followed in this thesis to find a solution for the above mentioned research questions.

1. Dynamic modelling of the induction motor with stator inter-turn fault using reference frame theory in the MODELS environment of EMTP, version

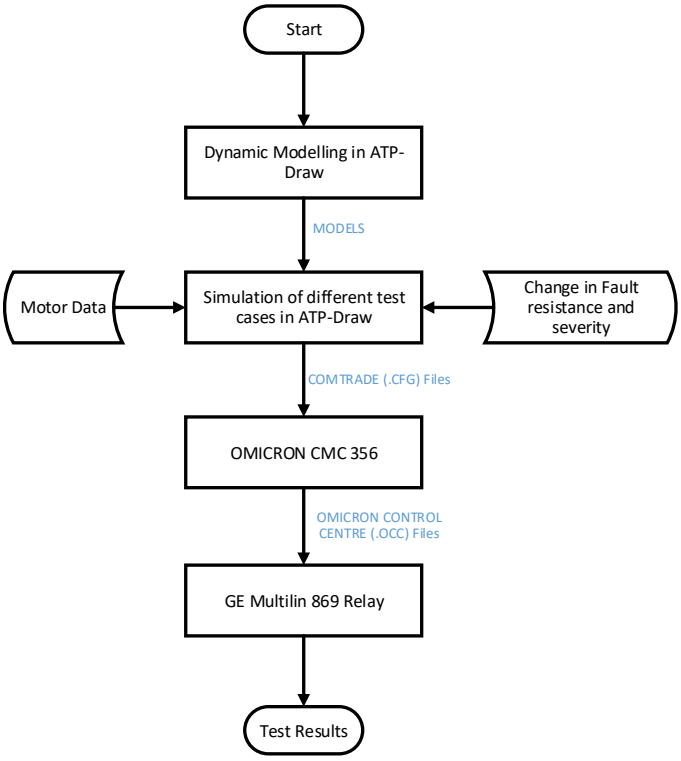

Figure 1.2: Flowchart describing the thesis objectives

ATPDraw.

2. Simulation of different test cases by varying fault resistance & severity to obtain the output voltage and current plots in ATPDraw. These output waveforms are measured at the secondary terminals of current and potential transformers and are exported in Common format for Transient Data Exchange (COMTRADE) (.CFG) format.

3. Replication of excitation behaviour from the exported waveforms to the relay using a secondary injection test kit, the OMICRON CMC 356.

4. Testing of the GE Multilin 869 motor protection relay using the OMICRON CMC 356 test kit.

5. Analysis of test results for all the defined test cases and recommend opti-

mal settings for the relay.

1.4. Previous Work

Prior to this project, a numerical relay, Siemens Siprotec 7SJ645 motor protection relay was considered for detection of stator inter-turn faults. The principle of protection used in this relay is based on negative sequence overcurrent protection and different characteristics associated with it. This numerical relay implements sequence filter to calculate the symmetrical components from the phase quantities. This relay offered different types of protection settings. For an accurate detection, two characteristics of overcurrent protection were considered: definite time and inverse.

2

Modelling of Induction Motor

Induction motors are available in a varied range of voltages and sizes. Small single phase induction motors majorly find its use in domestic appliances such as blenders, lawn mowers, washing machines etc. Large three phase induction motors are installed in pumps, fans, compressors and similar applications. A linear version of the induction motor is specifically designed for transportation system.

2.1. Equivalent circuit of an Induction Motor

The working principle of an induction motor is based on the Faraday's law of electromagnetic induction in which Electromotive Force (EMF) are induced across electrical conductors when they are placed in a rotating magnetic field. The two essential components of the induction motor are stator and rotor. The stator is a stationary part and is composed of high grade steel laminations. The inner frame of the stator consists of slots that carries the overlapping windings. In a three phase motor, these windings are physically placed 120°apart to maintain a sinusoidal nature. The rotor is the rotating part and is composed of ferro-magnetic material, with slots on it's outer surface that carries the field windings. Based on the type of windings in the rotor, induction motors can be of two types, *squirrel-cage* or *wound-rotor* type. In a squirrel-cage type rotor, the windings at the ends are shorted using end rings, whereas in a wound-rotor type, the terminals of the windings are closed through an external resistance. Since, a squirrel-cage type motor requires less maintenance, is simple and economical, it is a preferred option in the industry

Based on the Lenz's law, the direction of rotation of the rotor is along the rotating field such that the relative speed between the field and the winding decreases. The rotor will eventually reach a steady-state speed n which is less than

2

the synchronous speed n_s which is the speed of the rotating field. The rotor never reaches the n_s as it has to maintain a relative motion between the rotating magnetic field and the stationary conductors. The relative motion induces an EMF in the rotor. If this relativity is not achieved, no emf is induced and hence no induced current in the rotor to produce torque. The difference between the rotor speed n and the synchronous speed n_s is known as *slip (s)* and is defined as :

$$s = \frac{n_s - n}{n_s}$$

Generally, the value of slip at full load varies from less than 1% in high power motors to less than 2% in small motors. An induction motor can be represented as a circuit model which includes elements like stator and rotor impedance, and mutual reactance. The linking of the stator and rotor circuits can be considered as an ideal generalised transformer in which the standstill rotor voltage and rotor current are linked to the stator via a transformation ratio *a*. In the equivalent circuit, the rotor impedances are referred to the stator side using this transformation ratio. The frequency of the motor appears in the rotor through slip *s*. Therefore, in the equivalent circuit, the rotor impedance is referred to the stator side in two-step method: transformation using turn ratio and then frequency transformation to the stator frequency. The per-phase equivalent circuit of the transformed induction motor is as depicted in the Figure 2.1.

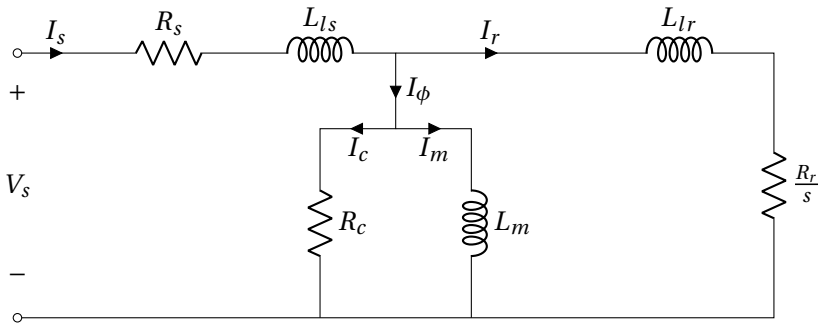

Figure 2.1: Equivalent circuit of an induction motor

where,

V_s : Stator Voltage
I_s : Stator Current
I_r : Rotor Current
R_s : Stator Resistance
L_{ls} : Stator Leakage Inductance
R_c : Core loss Resistance
L_m : Magnetising Inductance
R_r : Referred Rotor Resistance
L_{lr} : Referred Rotor Leakage Inductance

The equivalent circuit model can assume a form similar to that of an transformer. The stator circuit is similar to that of the primary side of a transformer and the rotor circuit, when represented from the point of view of stator side, represent the secondary side when referred to the primary side. The difference lies in the magnitude of some parameters. For example, the excitation current, I_ϕ, is as high as 30% to 50% of the rated current, whereas it lies between 1% to 5% in transformers. Similarly, the leakage reactance of an induction motor is substantially higher than that of a transformer due to the air gap and because the stator and rotor windings are distributed along the periphery of the air gap whereas in a transformer, it is concentrated on it's core.

Induction motors have nearly constant-speed characteristics with variation in loads. The air-gap flux in the induction motor is solely generated based on the stator excitation. The torque developed in an induction motor is dependent on the induced current in the rotor which runs at a non-synchronous speed; hence, the name asynchronous. Unlike induction motors, the synchronous machine requires an additional field excitation in the rotor. The torque developed in synchronous machine is dependent on the locking of fields of stator and rotor which occurs at synchronous speed. Therefore, induction motors remain unperturbed by the stability issue which is inherent to the synchronous machines that operate only at a single speed.

2.2. Dynamic Modelling of Induction motor

An accurate modelling of an induction motor is important to aid in fault prediction and detection. There are multiple ways to develop an induction motor with fault. The most commonly used methods are:

- Modelling based on dynamic equations of the motor with additional current loops representing the fault.
- Finite element modelling of the motor with modifications in the geometry to accommodate the fault.

In this thesis, the motor along with the stator inter-turn fault is modelled based on the dynamic equations. The models developed by Williamson *et al.*, Kliman *et al.*, and Luo *et al.* mimic the behaviour of an induction motor with stator inter-turn fault. However, they do not consider the non-linearities involved and fail to accurately detect these faults. Therefore, a more observant and vigilant model has to be considered to avoid false trips [5]–[7].

To develop a working model of an induction motor, classical voltage and torque equations expressed in terms of the motor parameters are used. These equations represent the steady-state and the dynamic performance of the motor.

It is difficult to incorporate all the non-linearities that exist in an actual motor. Therefore, certain assumptions and hypotheses are considered to develop a working mathematical model with fewer complexities. These assumptions are listed below:

- The stator windings are symmetrically placed 120° apart such that they are sinusoidally distributed on the periphery of the stator.
- The stator inner side is smooth i.e. the effects of the slots are neglected.
- Phenomena such as hysteresis, eddy-currents, skin-effect, saturation etc. are neglected.
- Spatial Magnetomotive Force (MMF) harmonics are neglected.
- The iron parts are considered to be infinitely permeable.
- The magnetic field intensity remains constant and is directed radially along the air gap.
- The mathematical model parameters do not vary with change in temperature of the motor.

The resulting stator and rotor voltage equations of the induction motor in vector form are :

$$\begin{aligned} V^s_{abc} &= R_s i^s_{abc} + \frac{\mathrm{d}\lambda^s_{abc}}{\mathrm{d}t} \\ 0 &= R_r i^r_{abc} + \frac{\mathrm{d}\lambda^r_{abc}}{\mathrm{d}t} \end{aligned} \tag{2.1}$$

where,

V^s_{abc} : Stator Voltages in 'abc' frame
i^s_{abc} : Stator Currents in 'abc' frame
R_s : Stator Resistance
λ^s_{abc} : Stator Flux-Linkages in 'abc' frame
i^r_{abc} : Rotor Currents in 'abc' frame
R_r : Referred Rotor Resistance
λ^r_{abc} : Rotor Flux-linkages in 'abc' frame

2.2.1. Transformation Theory

The coefficients of the voltage equations that describe the behavior of the motor are time varying in nature. These coefficients determine the motor impedances and are functions of the rotor speed. Therefore, to reduce the complexity of these equations, the involved variables are transformed and treated differently. The transformation refers the motor variables to a frame of reference that rotates at an arbitrary angular speed [8].

Based on the speed of rotation of the reference frame, well known transformations such as Park's transformation, Clarke's transformation, etc. are used. These transformations eliminate the time-varying inductances by referring the stator and rotor variables to a single reference frame that may rotate at a defined angular speed.

2.2.2. Choice of Reference Frame

The choice of angular speed determines the state of the reference frame. Both the stator and rotor variables are referred to the reference frame rotating at chosen angular speed. For modelling the induction motor, the choice of reference frame plays an important role. Three most commonly used reference frames are tabulated in Table 2.2.

Table 2.1: Commonly used reference frame

Reference frame speed	**Interpretation**
0 (Stationary)	Stationary circuit variables referred to a stationary reference frame
ω_r (Rotor)	Stationary circuit variables referred to a reference frame fixed in rotor
ω_s (Synchronous)	Stationary circuit variables referred to a synchronously rotating reference frame

When the three-phase quantities are transformed from three-phase reference frame to a two-axis orthogonal stationary reference frame, it is known as

Clarke's transformation. In this transformation, the two stationary two-phase variables are denoted as α and β which are orthogonal to each other. Furthermore, the resulting two-phase orthogonal quantities can be transformed to a rotary reference frame with arbitrary angular speed, which is known as Park's transformation.

2

For convenient modelling of the induction motor in this thesis, the stationary reference frame is chosen i.e. Clarke's transformation. A power invariant form of this transformation is used to transform all the stator and rotor variables into its respective α and β components using the transformation matrix X_{dq0}.

$$X_{dq0} = \sqrt{\frac{2}{3}} \begin{bmatrix} \cos(\omega t) & \cos(\omega t - 2\pi/3) & \cos(\omega t + 2\pi/3) \\ -\sin(\omega t) & -\sin(\omega t - 2\pi/3) & -\sin(\omega t + 2\pi/3) \\ 1/\sqrt{2} & 1/\sqrt{2} & 1/\sqrt{2} \end{bmatrix} \begin{bmatrix} X_a \\ X_b \\ X_c \end{bmatrix} \tag{2.2}$$

The transformed variables can be restored to their original form by using the inverse transformation matrix X_{abc}.

$$X_{abc} = \sqrt{\frac{2}{3}} \begin{bmatrix} \cos(\omega t) & -\sin(\omega t) & 1/\sqrt{2} \\ \cos(\omega t - 2\pi/3) & -\sin(\omega t - 2\pi/3) & 1/\sqrt{2} \\ \cos(\omega t + 2\pi/3) & -\sin(\omega t + 2\pi/3) & 1/\sqrt{2} \end{bmatrix} \begin{bmatrix} X_d \\ X_q \\ X_0 \end{bmatrix} \tag{2.3}$$

Based on the transformation presented in (2.2), the voltage equations in (2.1) are transformed as follows:

$$\begin{aligned} V_{ds} &= R_s i_{ds} - \omega \lambda_{qs} + \frac{\mathrm{d}\lambda_{ds}}{\mathrm{d}t} \\ V_{qs} &= R_s i_{qs} + \omega \lambda_{ds} + \frac{\mathrm{d}\lambda_{qs}}{\mathrm{d}t} \\ V_{qr} &= R_r i_{qr} + (\omega - \omega_r)\, \lambda_{dr} + \frac{\mathrm{d}\lambda_{qr}}{\mathrm{d}t} \\ V_{dr} &= R_r i_{dr} - (\omega - \omega_r)\, \lambda_{qr} + \frac{\mathrm{d}\lambda_{dr}}{\mathrm{d}t} \end{aligned} \tag{2.4}$$

From the above-mentioned equations, the flux-linkages are defined as follows:

$$\begin{aligned} \lambda_{ds} &= L_s i_{ds} + L_m i_{dr} \\ \lambda_{qs} &= L_s i_{qs} + L_m i_{qr} \\ \lambda_{dr} &= L_r i_{dr} + L_m i_{ds} \\ \lambda_{qr} &= L_r i_{qr} + L_m i_{qs} \end{aligned} \tag{2.5}$$

where L_s and L_r are the stator and rotor inductance respectively, and are defined as follows:

$$L_s = L_{ls} + L_m$$
$$L_r = L_{lr} + L_m \tag{2.6}$$

where,

V^s_{dq}	:	Transformed Stator Voltages
i^s_{dq}	:	Transformed Stator Currents
R_s	:	Stator Resistance
L_s	:	Stator Inductance
λ^s_{dq}	:	Transformed Stator Flux
i^r_{dq}	:	Transformed Rotor Currents
R_r	:	Referred Rotor Resistance
L_r	:	Referred Rotor Inductance
λ^r_{dq}	:	Transformed Rotor Flux-linkages
ω	:	Rotational Frame Speed
ω_r	:	Rotor Speed

2.3. Simulation in ATP-Draw

To predict the dynamic performance of an induction motor, it is simulated digitally. The primordial models used the *exact equivalent circuit* to represent an induction motor. These models used lumped circuit model parameters as they were based on the concept of magnetically coupled circuits. But these models did not include certain phenomena such as motor start up. Therefore, with relevant research in the digital computing, changes were made to the modelling technique and circuit models are generated with more accuracy.

Various digital computer programs are used to simulate ac motors and determine their dynamic performance and transient phenomena. In this thesis, EMTP-ATP is used. It is a program developed dedicated to study the potential problems in an electrical power system. This program helps characterise transient events as they have a wide range of modelling capabilities and simulate them within few microseconds.

EMTP-ATP has a default component known as "universal machine" that contains majority of the functions of an induction motor. This component requires very little information about the motor for its operation as an induction motor. This model is designed based on "direct-quadrature axes" theory. The internal modelling requires the following information about the motor:

- Stator Resistance (R_s)
- Referred Rotor Resistance (R_r)
- Magnetising Inductance (L_m)

- Stator Leakage Inductance (L_s)
- Referred Rotor Leakage Inductance (L_r1)
- Moment of Inertia (J)
- External Load torque (T_L)

These parameters are determined by EMTP's Universal Induction Machine with Manufacturer's Data Input (UMIND) model that uses the nameplate data as input. The fit of the determined parameters can be increased by changing the weight of each data input given to the model. To obtain the best fit for the motor parameters, the rated current should match the data sheet. The universal machine model is an in-built model with pre-defined functions. It cannot simulate transients such as winding faults. Therefore, for this thesis, the induction motor was simulated using MODELS. The stator inter turn fault was also designed in this model.

MODELS is a user-defined tool in ATP that describes the dynamic behaviour of complex physical systems such as the working of circuit & control components. The motivation of using MODELS in ATP is [9]:

1. To develop models of elements, phenomena and motors that are not available in the existing libraries.
2. To set initial states, history and working of a component at any level of detail.
3. To be able to communicate with external programs at the modelling level with voltage, current and control signals.

For this thesis, the structure followed for the developing a dynamic model of an induction motor with a stator inter-turn fault is tabulated in Table 2.2 [10]. The developed model is presented in Appendix B.

The syntax and functions used in this MODELS are with reference to the user guide defined by EMTP [9]. The resulting induction motor model is as shown in the Figure 2.2.

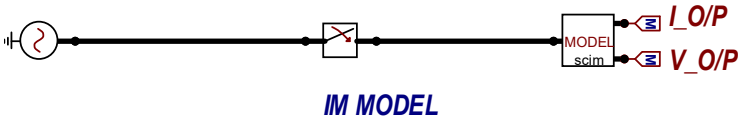

Figure 2.2: Simulated Induction Motor in ATPDraw.

Table 2.2: Procedure used in MODELS in ATP

DATA	• Source Parameters, • Equivalent motor Parameters, • Rated Frequency.
VARIABLES	• Terminal Phase and transformed Voltages and Currents, • Electrical quantities such as ω_r, ω_r, fluxes, fault quantities • Mechanical quantities such as torque, rotor position.
HISTORY	• Declaration of past values
INITIALISATION	• Peak values of input voltage, • Initialise all the motor parameters at t=0.
EXECUTION	• Calculation of terminal voltage in phase and transformed quantities, • Solving of steady-state equations including startup • Simulation of stator inter-turn fault after steady-state of the motor, • Determination of the rotor speed and angle • Obtain the actual variables after inverse transformation.
OUTPUT	• Obtain resulting voltages and currents.

The induction motor in focus is part of a power system network as shown in Figure 2.3. The parameters of this induction motor used in this research is as given in the Table 2.3.

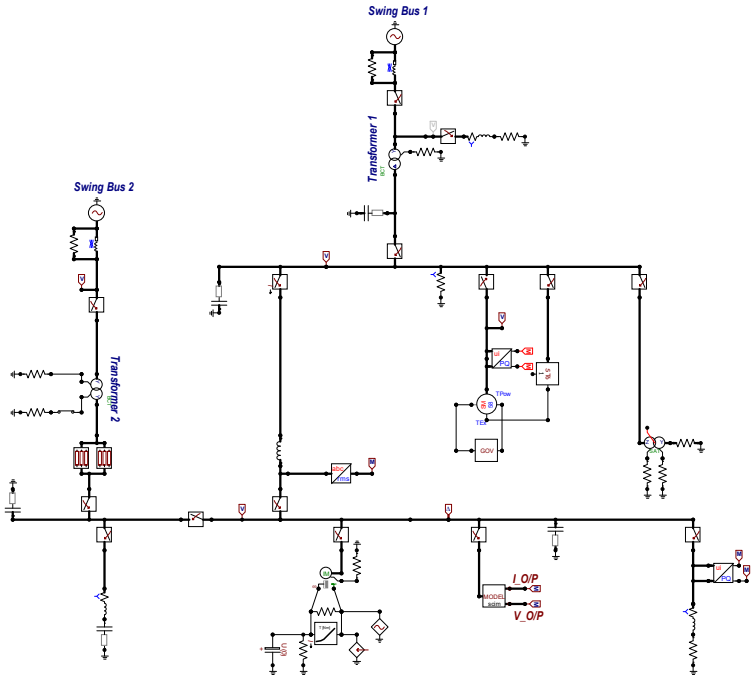

Figure 2.3: Network of which the induction motor is part of

2.4. Validation of the Developed Model

The validation of the developed model is done by comparing the electrical torque and the load current with that of universal model and manufacturer data sheet. The validation model (Figure 2.4) consists of a voltage source of 6.3 kV and a switch that operates the motor. The electrical torque is modelled to match the loading of the equipment. An induction motor is represented mathematically to integrate all the elements of electromagnetic and mechanical parts of the motor.

The Universal module in EMTP represents the mechanical parts of an induction motor as its equivalent electrical components. Table 2.4 tabulates the equivalent representation of these components. The rules followed to establish the equivalence between the mechanical and electrical components is as given below [11]:

Table 2.3: Machine Parameters of the modelled induction motor

Parameter	Value
Stator Resistance (R_s)	0.797 Ω
Stator Leakage Inductance (L_s)	5.592 mH
Rotor Resistance (R_r)	0.1957 Ω
Rotor Leakage Inductance (L_r)	5.592 mH
Mutual Inductance (L_m)	281.638 mH
Power	2025 Hp (1510 kW)
Voltage	6.3 kV
Nominal Current	160 A
Rated Speed	2973 rpm (311 rad/s)
Pole Pairs	1

- In the equivalent network, the moment of inertia is represented as a node with a capacitor to ground for the mass of the shaft.
- In the equivalent network, a current source is connected to the mass node upon which mechanical torque is acting.
- The damping proportional to the speed is represented as a resistor in parallel to a capacitor.
- Two or more masses are represented as inductors.
- Damping associated to coupling is represented as inductor in parallel to a resistor.

Table 2.4: Equivalent representation between mechanical and electrical components [11]

Mechanical Parameter	Electrical Representation
Torque acting on mass (T)	Current into a node (i)
Angular Speed (ω)	Node Voltage (v)
Angular position (θ)	Capacitor Charge (q)
Moment of inertia (J)	Capacitance to ground (C)
Spring Constant (K)	Reciprocal of Inductance ($1/L$)
Damping Coefficient (D)	Conductance (G)

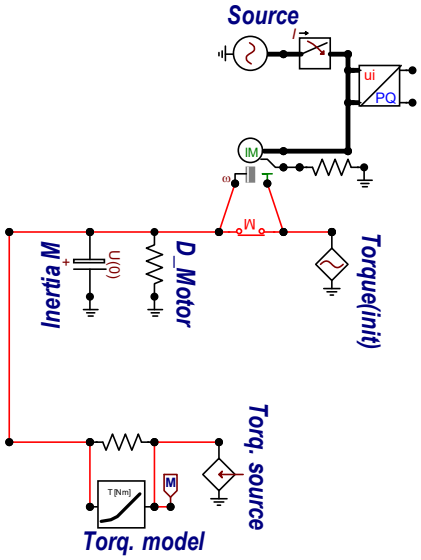

Figure 2.4: Model used to validate the developed model

The torque is modelled based on the polynomial given as $A_0 + A_1 \times \omega + A_2 \times \omega^2 + A_3 \times \omega^3$. The coefficients A_0, A_1, A_3 are considered to be 0 and A_2 is 0.73 based on the loading of the motor.

It can be observed that the torque (Figure 2.5) and speed (Figure 2.6) plots are similar implying the developed model in MODELS environment is comparable to the default universal motor model in EMTP.

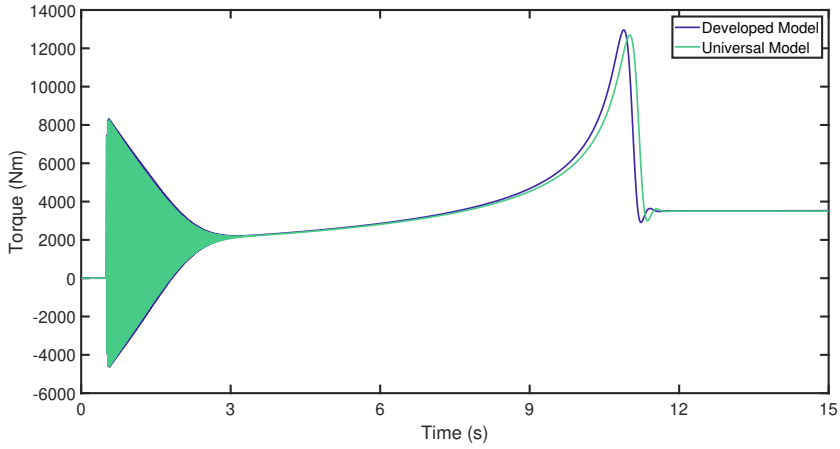

Figure 2.5: Comparison of torque plots between the developed and the universal model

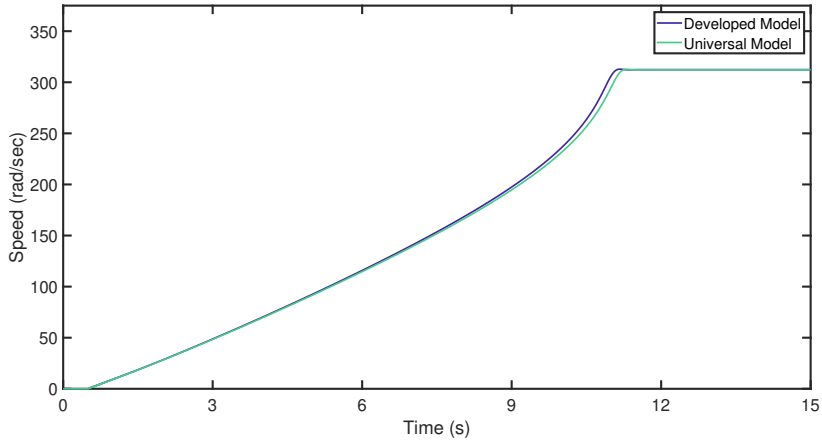

Figure 2.6: Comparison of speed plots between the developed and the universal model

3

Stator Inter-Turn Faults

Petrochemical industries, refineries, and gas terminals are filled with chemicals and explosives content. This is a tough environment for electrical equipments to operate. The rugged construction of an induction motor helps it to endure these rough environments. However, the induction motor fails due to a variety of stresses upon the motor.

These stresses on the motor can be classified into the following:

- Stator Stresses
- Bearing Stresses
- Shaft Stresses
- Rotor Assembly Stresses.

With frequent occurrence of failures in the induction motor, the establishment gets affected due to unprecedented halts in their operation. These halts largely affect the establishment economically. The survey conducted by Penrose estimates the average downtime cost of the motor failures in different industries as tabulated in Table 3.1 [12].

3.1. Causes of Stator Inter-turn Faults

The prime cause of stator inter-turn fault is insulation degradation due to failures caused by electrical, thermal and mechanical stresses. This degradation leads to flow of current which is higher than leakage current through an unintended path created due to the reduced insulation resistance. These currents create new current loops leading to excessive heating in the machine. This additional heating

Table 3.1: Estimation of Downtime Costs [12]

Industry	Average Downtime Cost ($/hour)
Forest	7,000
Food processing	30,000
Petro-Chemical	87,000
Metal Casting	100,000
Automotive	200,000

expedites the process of insulation degradation [13]. Overvoltage stresses is the most probable cause of electrical and thermal stresses on the machine. The voltage gradient across a winding is highest at the first few turns. Therefore, the occurrence of stator inter-turn fault at these locations is highly probable. Mechanical and chemical stresses can also be responsible for insulation degradation. An induction machine in a contaminated environment is susceptible to pollutants that may affect the insulation between turns by creating a path for small currents to flow [14].

3.2. Consequences of Stator inter-turn faults

A stator inter-turn fault is generally a consequence of combination of stresses: ageing, contamination, exposure to chemical substances, moisture, heat, large transients in the motor. The fault starts with a degradation of the insulation material leading to breakdown of adjacent turns' insulation and thus leading to incipient stator inter-turn short circuit fault [15].

The effect of an inter-turn fault on an induction motor is as follows [16]:

1. The fault creates asymmetries in the balanced three phase circuit which results in varying amplitudes of stator current.

2. The fault increases the harmonics in the air gap flux, breaks the symmetric magnetic line of force and increases the saturation degree of magnetic density with deepening of fault severity.

3. The fault introduces ripples in the electromagnetic torque. These ripples increase with growing fault severity which affects the operational stability of the system.

4. The fault creates localised heating which can be proved dangerous in industries with volatile work environment.

Ideally the insulation resistance is infinite and the fault current is zero before the fault is incepted. However, with the degradation of the insulation material, the insulation resistance tends to zero and value of fault current increases. The effective turns on the faulty phase are reduced during the fault. This reduction affects the MMF induced in the healthy section. Along with the reduced MMF, the fault current produces MMF in the opposite direction that weakens the existing one in the faulty phase.

The faulty phase can be considered as an auto transformer where the entire phase is the primary side while the faulty part is the secondary. Subsequently, high currents are induced in the secondary side based on the transformation ratio:

$$\frac{N_1}{N_2} = \frac{I_2}{I_1}$$

The fault current causes abnormal heating and spreads to the surrounding windings resulting in a sequential phase to ground or phase to phase fault. Hence, timely detection of the stator inter-turn fault can prevent severe damages and huge downtime of the motor. But, the fault current is not reflected at the stator terminals which becomes a challenge in the detection of the fault.

3.3. Stator Inter-turn Fault Detection Techniques

A stator winding fault starts with failure of insulation between two turns in a phase of the stator. The shorted turn affects the surrounding turns leading to a insulation failure in the stator. The faulty turns generate circulating current which increases the temperature in the affected area as the machine continues to operate. The increased temperature may further damage the insulation of the neighbouring areas.

The occurrence of inter-turn fault can propagate to larger sections of the winding resulting into a coil-to-coil short circuit or phase-to-phase short circuit [17]. Figure 3.1 represents different types of possible stator failure modes. These faults can further develop into phase-to-ground faults causing significant damage to the machine. Such failures can cause large fault current, resulting in irreversible damage to the machine [13].

The main cause of such failures can be accounted for the different types of stress i.e. mechanical, thermal, electrical, and environmental the machine undergoes during its operating life. The increased prevalence of the fault makes it a pressing matter to identify and adopt diagnostic techniques to avoid further failures. If they go undiagnosed, reduced efficiency, increased costs and reduced operating life can be expected. Continuous development in the sector of the digital signal processing and sensing helps researchers to develop monitoring and testing techniques for inter-turn faults. These techniques rely on non-invasive

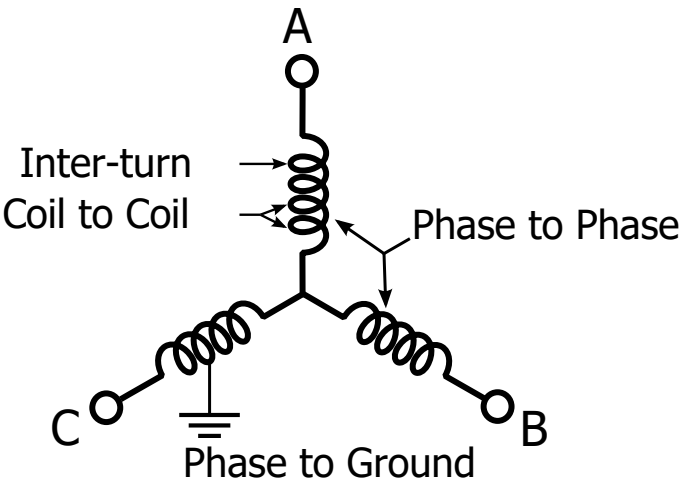

Figure 3.1: Representation of possible stator failure modes [18].

monitoring and analysing electromagnetic and electrical quantities such as flux, terminal current, voltage and equivalent impedance. Fault detection and prediction methods can be used to prevent these failures and reduce corollary financial losses.

Over the years, various studies have been carried out on effective fault monitoring and diagnosis methods based on the common processes followed in the industry. The monitoring and detection methods can be broadly categorised into five groups [19]:

- Sound and Vibration Analysis: A stator winding fault was detected and diagnosed using acoustic signal in a single phase induction machine. This method had a success of 88% in the study [20]. Based on this study, diagnostic methods continued using sound and vibration signals to detect winding faults [21]. These studies established a coherent relationship between motor currents and vibrations that is used as an indicator of internal faults.

- Air gap Torque Analysis: An unbalanced voltage can cause harmonics in the air gap torque of an induction motor. These harmonics affect the torque, magnetic flux and the power factor of the machine. As a result, they create pulsating speed, vibrations and noise causing deterioration in the insulation [22]. The vibration signals and the magnetic flux of the induction motors was used to diagnose stator faults [23].

- Current Analysis: The occurrence of a fault in the induction motor induces

harmonics in the stator current. Therefore, a lot of studies use current signatures to analyse and detect discrepancies in the machine. This is a preferred method as the stator current is easily accessible while the machine is operational [24]. However, the accuracy of the technique is affected by the load factor of the machine and the signal to noise ratio.

The most reliable current phase to be selected for this technique in a $3-\phi$ machine is chosen using fuzzy entropy technique. The chosen phase is then given as an input to artificial neural networks where the faults are investigated using Fourier and wavelet transformation [25]. Different techniques use different strategies on the current signals, such as Hilbert transformation, Park vector Product Approach, to detect the fault [26].

- Temperature Analysis: A major cause of failure of induction motors is overheating. Protective devices such as fuses, thermal switches and relays are used to protect the network from possible thermal faults. Detection of an internal fault can be performed by monitoring the temperature. The temperature can be observed using sensors installed in the protection scheme of the motor.

  Rajagopal *et al.* used heat transfer coefficients of the induction machine model to study a two-dimensional thermal transient analysis in his study to detect internal faults in the stator [27]. The thermal images received from the model are analysed using a method called Method of Area Selection of States in which the feature vectors are reconstructed based on a predefined mathematical model and fault location is determined [20].

- Magnetic flux Analysis: Under normal conditions, the magnetic flux in the air gap of an induction machine is sinusoidal in nature. But with the occurrence of a fault in the stator, the air gap flux density changes resulting in unbalanced voltages. The continuous sensing of voltage is achieved using a search coil positioned around the shaft. This technique is highly efficient at full load conditions.

A few other detection techniques include partial discharges and artificial intelligence. In case of partial discharge in motor insulation, a byproduct is ozone. The resulting ozone can be used as indicator for insulation failure [28]. This technique requires additional equipments such as as optical sensor for detection of ozone which is an additional investment. Artificial intelligent tools such as neural networks, genetic algorithms, wavelet analysis of current and voltage signals can be implemented as detection techniques. These techniques allow the user to detect the fault online with a minimum prior knowledge.

In this thesis, the fault detection technique is based on the analysis of negative sequence component of the fault current. Techniques that involve sequence components are susceptible to false diagnosis as the machine contains inherent imbalances [29]. Therefore, further researches were conducted to improvise this drawback. The more recent techniques use sequence impedances, which is the ratio of negative sequence voltage over the negative sequence current as and index to overcome the effects of inherent asymmetries of the machine [14].

3.4. Modelling of Stator Inter-turn fault

Considering the inter-turn fault is on phase A, the windings are divided into two parts: shorted and healthy turns as shown in Figure 3.2.

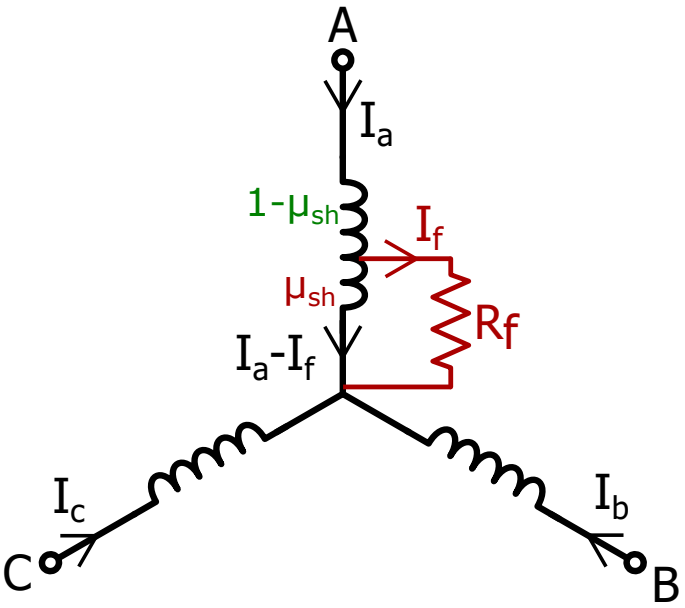

Figure 3.2: Representation of inter-turn fault in phase-A

I_a, I_b, I_c,	:	Phase Currents
μ_{sh}	:	Fault Severity
R_f	:	Fault Resistance
I_f	:	Fault Current

The impedances of the shorted winding is proportional to μ_{sh} that represents the effective number of faulty turns. The fault is mathematically modelled in line with [30] and [31]. Therefore, the voltage and flux-linkage equations of stator and rotor can be written as:

$$
\begin{aligned}
V^s_{abc} &= R_s\left(i^s_{abc} - \mu_{abc} I_f\right) + \frac{\mathrm{d}\lambda^s_{abc}}{\mathrm{d}t} \\
V^r_{abc} &= R_r i^r_{abc} + \frac{\mathrm{d}\lambda^r_{abc}}{\mathrm{d}t} \\
R_f i_f &= R_s \mu_{sh}\left(i^s_a - i_f\right) + \frac{\mathrm{d}\lambda^{sh}_a}{\mathrm{d}t}
\end{aligned} \tag{3.1}
$$

$$
\begin{aligned}
\lambda^s_{abc} &= L_s\left(i^s_{abc} - \mu_{abc} i_f\right) + L_m i^r_{abc} \\
\lambda^r_{abc} &= L_m\left(i^s_{abc} - \mu_{abc} i_f\right) + L_m i^r_{abc}
\end{aligned} \tag{3.2}
$$

The Clarke transformation mentioned in section 2.2 is used to transform the above-mentioned voltage and flux-linkage equations into the $\alpha\beta$ reference frame. The equivalent circuits and the respective voltage and flux-linkage equations in the $\alpha\beta$ reference frame are presented below.

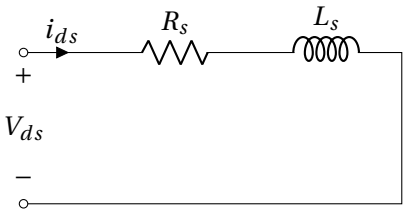

Figure 3.3: Stator equivalent circuit in d-axis

$$V_{ds} = R_s i_{ds} + \frac{\mathrm{d}\lambda_{ds}}{\mathrm{d}t} \tag{3.3}$$

$$\lambda_{ds} = L_s i_{ds} + L_m i_{dr} \tag{3.4}$$

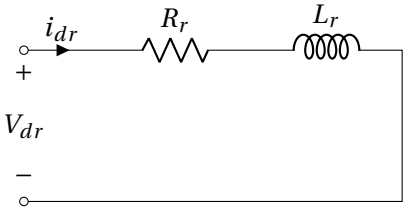

Figure 3.4: Rotor equivalent circuit in d-axis

$$0 = R_r i_{dr} - \omega_r \lambda_{qr} + \frac{\mathrm{d}\lambda_{dr}}{\mathrm{d}t} \tag{3.5}$$

$$\lambda_{dr} = L_r i_{dr} + L_m i_{ds} \tag{3.6}$$

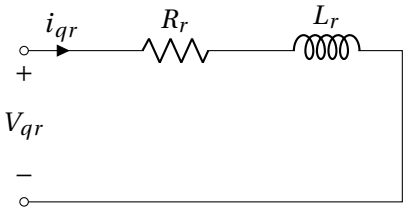

Figure 3.5: Rotor equivalent circuit in q-axis

$$0 = R_r i_{qr} - \omega_r \lambda_{dr} + \frac{\mathrm{d}\lambda_{qr}}{\mathrm{d}t} \tag{3.7}$$

$$\lambda_{qr} = L_r i_{qr} + L_m i_{qs} - \sqrt{\frac{2}{3}}\mu_{sh} L_m i_f \tag{3.8}$$

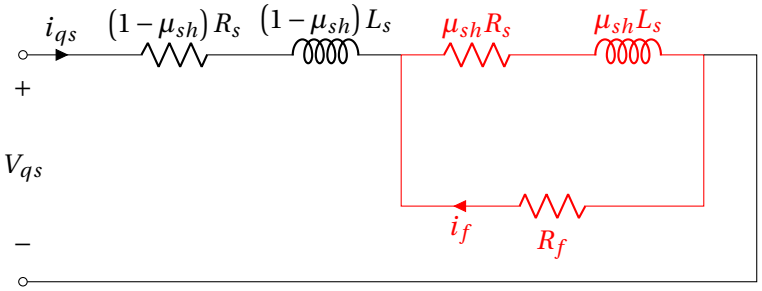

Figure 3.6: Stator equivalent circuit in q-axis

$$V_{qs} = R_s\left(i_{qs} - \sqrt{\frac{2}{3}}\mu_{sh} i_f\right) + \frac{\mathrm{d}\lambda_{qs}}{\mathrm{d}t} \tag{3.9}$$

$$\lambda_{qs} = L_s i_{qs} + L_m i_{qr} - \sqrt{\frac{2}{3}}\mu_{sh} L_s i_f \tag{3.10}$$

$$R_f i_f = \mu_{sh} R_s\left(i_{qs} - i_f\right) + \frac{\mathrm{d}\lambda_q^{sh}}{\mathrm{d}t} \tag{3.11}$$

$$\lambda_q^{sh} = \mu_{sh} L_{ls}\left(i_{qs} - i_f\right) + \mu_{sh} L_m\left(i_{qs} + i_{qr} - \sqrt{\frac{2}{3}}\mu_{sh} i_f\right) \tag{3.12}$$

The electromagnetic torque of the motor can be expressed as:

$$T_{em} = \frac{3}{2}\frac{P}{2} L_m\left(i_{qs} i_{dr} - i_{ds} i_{qr}\right) - \frac{P}{2} L_m \mu_{sh} i_f i_{qr} \tag{3.13}$$

3.5. Operation of the Developed Model

According to the datasheet of the motor, its starting time is 10 seconds. Since, the start up performance of the motor falls out of scope in this work, the moment of inertia is scaled down by a factor of 10 during startup to achieve steady-state faster. The different operating conditions of the motor are:

Table 3.2: Operating condition of the motor

Time (s)	Operating Condition
0.5	Switch on
0.5 - 2.0	Startup
2.0 - 2.5	Steady-state
2.5 - 3.0	Fault condition

3.5.1. Terminal Current

The model is developed such that it simulates terminal currents for a period of 3.0 s. The stator terminal currents are as shown in Figure 3.7.

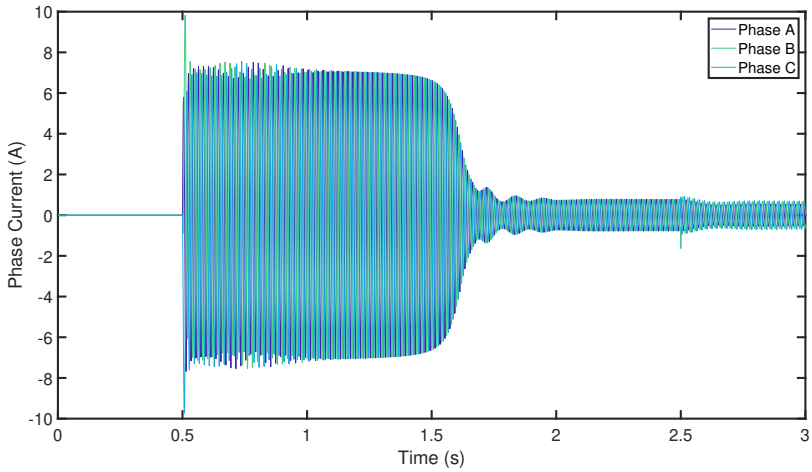

Figure 3.7: Stator terminal Currents

As noted in Table 3.2, the fault in the motor is initiated at 2.5 s. After this instance, the magnitude of terminal current does not vary much. This variation is not sufficient enough to be measured at the stator terminals by the conventional protection scheme. However, the fault creates an unbalance in the terminal cur-

rents that gives rise to negative sequence component. The symmetrical components of voltages and currents can be used for detection of this fault. Such imbalances also occur during the motor start-up. Therefore, proper differentiation is necessary to distinguish the two types of negative sequence components to avoid false trips.

3.5.2. Fault Current

Figure 3.8 plots the fault current flowing through the faulted windings during a stator inter-turn fault.

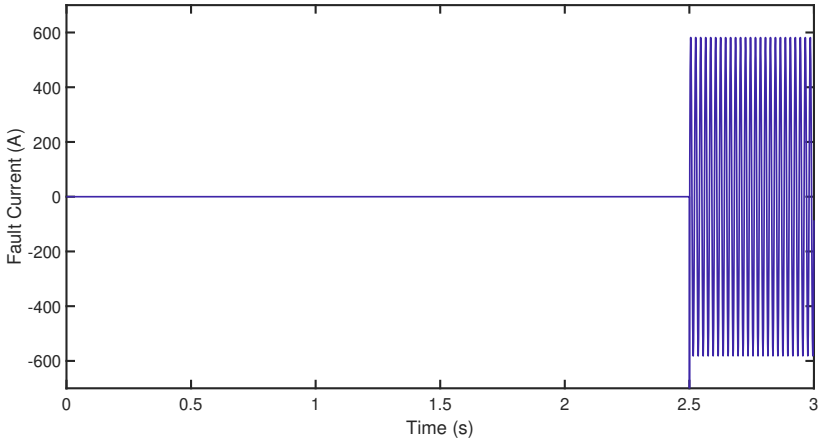

Figure 3.8: Fault Current

The magnitude of the fault current is dependent on two factors: fault resistance (R_f) and fault severity (μ_{sh}). As noticed in the Figure 3.8, the magnitude of fault current is not high as compared to a typical fault current. Therefore, it can be implied that this fault current is circulatory in nature. Continuous flowing of this current will lead to localised heating resulting in prolonged damages to the stator insulation. This can be avoided by timely detection of the stator inter-turn fault.

3.5.3. Electromagnetic Torque

The electromagnetic torque of the motor is as shown in Figure 3.9.

The asymmetrical terminal currents result in unbalanced air gap. The resulting MMF affects the induced EMF and currents in the rotor. The affected induced current creates fluctuations in the torque. These fluctuations increase with increasing fault severity.

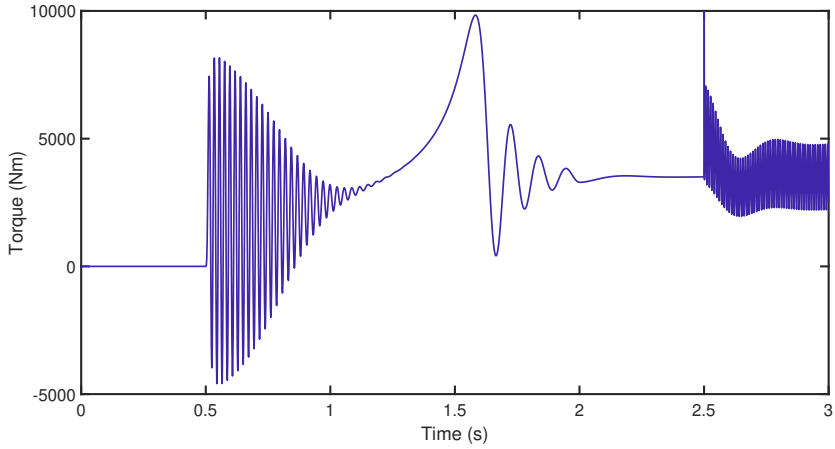

Figure 3.9: Fault Torque

3.5.4. Rotor Speed

Figure 3.10 plots the rotor speed of the induction motor. The dependence of rotor speed on the electromagnetic torque can be expressed by the equation:

$$\frac{d\omega_r}{dt} = \frac{1}{J}(T_{em} - T_L) \tag{3.14}$$

where,

ω_r : Rotor Speed
J : Moment of Inertia
T_{em} : Electromagnetic Torque
T_L : Load Torque

Due to this dependence, the fluctuations in the electromagnetic torque result in oscillating rotor speed. These oscillations reduce the speed from the rated full load speed. The speed plot shown in Figure 3.11 verifies the oscillations and the decrease in rotor speed. The magnitudes of oscillations are not significant because of high inertia of the induction motor.

Industries employ vibration monitoring schemes to detect any variations in the speed of the rotor. But the reduced oscillations as shown in Figure 3.11 are not detected by these systems. Therefore, a better detection scheme for stator inter-turn faults is required.

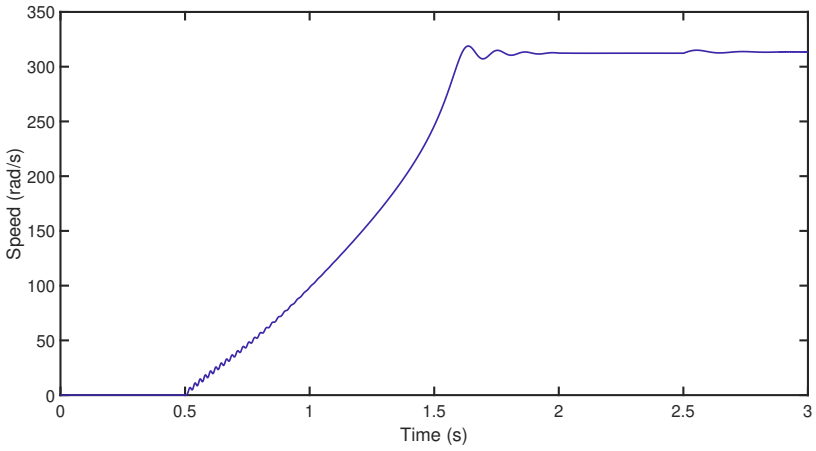

Figure 3.10: Rotor Speed

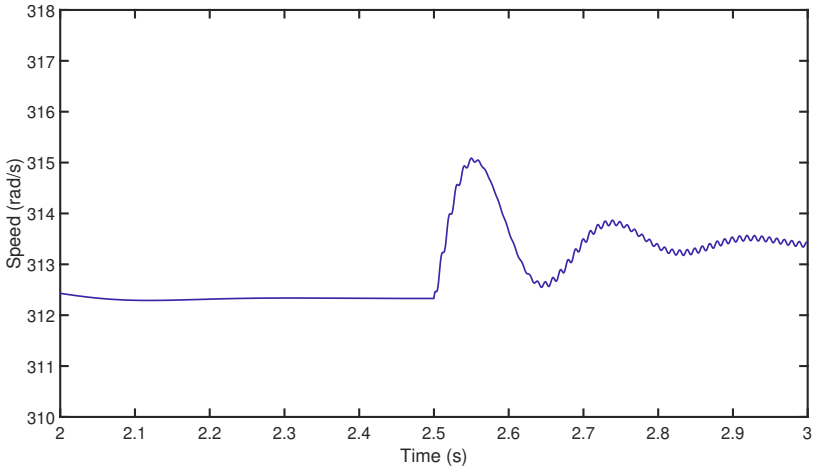

Figure 3.11: Ripples in rotor speed

4

Protection of the Machine

4.1. Protection Devices

Electrical equipment in a system may face intolerable conditions that can lead to failure of the responsible and neighbouring equipment. These conditions may be caused by natural phenomena such as lightning, or acts of human. Therefore, protective devices must be installed to ensure the reliability of the power system. They also limit the damage to the equipment preventing further progression of the fault.

Protective devices such as relays are compact intelligent electronic devices connected in different parts of a network to detect any abnormal operating condition. They monitor a defined signal which determines the state of system, and operate according to the settings of the device. They operate based on limits set on measured quantities such as voltage, current, current direction, power factor, power, impedances, temperature.

4.2. Principle of Motor Protection

Every machine is designed for specific operating conditions depending on the requirement and the functionality. When a machine exceeds these limits, it can lead to failure. Relays for motors are predominantly used in industries where the cost of replacement and maintenance of machines is higher than installation of protection relays. The schematic representation of a relay connection in a power system is as shown in Figure 4.1

where:

CB : Circuit Breaker
CT : Current Transformer
PT : Potential Transformer

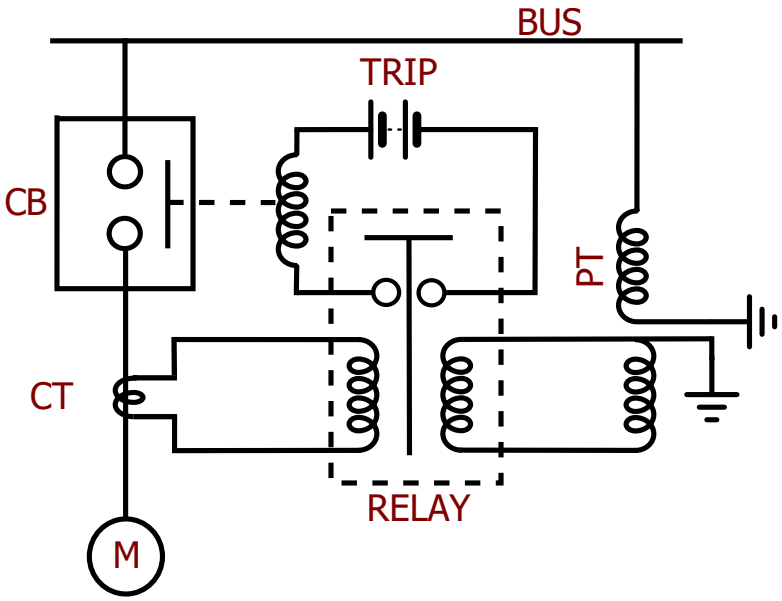

Figure 4.1: One line representation of a typical motor protection relay installation

Despite rugged construction of induction motors, its failures rate per year is significant. Conservatively, it can be estimated to 3 - 5 % per year. Some industries like chemical, mining, pulp and paper have motor failure rate up to 12%. All failures in the motor can be grouped into three categories: electrically related, mechanically related, environmentally related. Proper protection must be provided to the machine for each of these categories to ensure reliability and safety.

In an induction motor, protection is conventionally provided for common faults such as short circuits between phases or between phase and ground, unbalances between phases, and internal faults such as stator winding faults. These faults affect the system voltages and currents, and the change of these signals with respect to nominal values are detected by relays installed. Protection relays also prevent spreading of any disturbance due to these faults back to the network. Faults such as short circuits between phases or phases and ground result in high fault currents that can be easily detected by phase current measurement. However, faults such as stator winding faults do not result in high fault currents. Therefore, detection of these faults require additional computation to detect its presence.

When a stator inter-turn fault is not detected at an early stage, the fault current causes severe localised heating and can progress rapidly to a larger section of the winding, consequently leading to a phase to ground fault or phase to phase

fault. This forces the machine out of service and increases the downtime. In this project, GE Multilin 869 Motor Protection relay is considered to detect the presence of stator inter-turn fault.

4.3. GE Multilin 869 Motor Protection Relay

The GE Multilin 869 relay is a microprocessor based relay designed for protection of synchronous and asynchronous machines. This relay comprises of many novel features to match up to the industry standards and requirements. The features can be programmed individually to meet the user's needs. A brief list of all the functions available in the relay is as follows [32]:

- Motor Protection:
  - Differential
  - Thermal
  - Current Unbalance
  - Voltage Unbalance
  - Short Circuit
  - Overload
  - Ground Faults
- Synchronous Motor Protection:
  - Field Under/Over Current
  - Field Under/Over Voltage
  - SC Speed-Dependent Thermal
- 2-Speed Motor protection:
  - 2-Speed Thermal
  - 2-Speed Acceleration
  - 2-Speed Undercurrent
- Current Protection:
  - Phase/Neutral/Ground Time Over current
  - Phase/Neutral/Ground Instantaneous Over current
  - Phase/Neutral/Ground Directional Over current
- Voltage Protection:

  - Phase reversals
  - Under/Over voltages
  - Auxiliary Under/Over voltages
- Impedance protection
- Power:
  - Directional Power
  - Reactive Power
- Frequency Protection:
  - Under/Over Frequency
  - Rate of change of frequency

Relay setpoints are defined based on the information from the motor datasheets. If these information is unavailable, default values can be set for some functions during the commissioning.

The programming of these functions can be either be executed with the front panel keys and display screen on the relay or with a more interactive software called EnerVista 8 series Setup on a computer system. The software has two modes of working: online and offline. The online mode lets the user apply changes to the setpoints in real time whereas the offline mode allows to save relay settings in a file that can be uploaded to the relay at an later time.

4.4. Working Principle of the Relay

The Multilin 869 relay uses sequence components to provide advanced detection of stator inter-turn faults. A brief summary of sequence components is presented in Appendix A.

4.4.1. Methodology of Operation

The algorithm adopted in the relay can help detect an inter-turn fault before it progresses to insulation breakdown, reducing the unplanned downtime of the system.

In steady state, the sequence component voltage equation is given in Equation 4.1

$$\begin{bmatrix} V_1 \\ V_2 \end{bmatrix} = \begin{bmatrix} Z_{pp} & Z_{pn} \\ Z_{np} & Z_{nn} \end{bmatrix} \begin{bmatrix} I_1 \\ I_2 \end{bmatrix} \tag{4.1}$$

where,

V_1, V_2 : Positive and Negative sequence voltages
I_1, I_2 : Positive and Negative sequence currents
Z_{pp}, Z_{nn} : Positive and Negative sequence impedances
Z_{np}, Z_{pn} : Cross-coupled negative to positive/positive to negative sequence impedances.

In a symmetrical situation, the cross-coupled sequence impedances are zero implying that the positive and negative sequence components of the machine are decoupled. However, in practice, due to presence of inherent asymmetry in the circuit, the cross-coupled sequences impedances have a small value. The occurrence of a stator inter-turn fault further aggravates these values. The standardised ratio of cross-coupled impedances is an essential part in determining the operating condition of the relay. This ratio can be computed from the matrix given in Equation 4.1 and is given as [32]:

$$\frac{Z_{np}}{Z_{pp}} = \frac{V_2 - Z_{nn} I_2}{V_1}$$

The default value of the unbalanced impedance (Z_{UBbase}) is due to the inherent asymmetry in the machine and can be defined as [32]:

$$Z_{UBbase} = \left(\frac{Z_{np}}{Z_{pp}}\right) \text{at 0 inter-turn fault}$$

The relay has a learning phase where the algorithm learns the default unbalance impedance inherent to the machine (Z_{UBbase}) and uses this as a reference to determine the operating point (OP) as follows [32]:

$$OP = \frac{Z_{np}}{Z_{pp}} - Z_{UBbase}$$

The learning phase runs only once during the commissioning of the relay for given current transformers, potential transformers and machine ratings. A flowchart describing the phase is as shown in the. Once this phase is complete, the algorithm sets an average Z_{UBbase} value and moves to the monitoring phase. In this phase, the value of the operating point is zero during normal conditions and will be greater than zero during inter-turn fault conditions. The threshold to this operating point can be set to a near zero value to detect even a small percentage of shorted turns.

The characteristics of the algorithm used are [32]:

- the use of cross-coupled impedance.
- independent of load since the algorithm doesn't use positive sequence current.

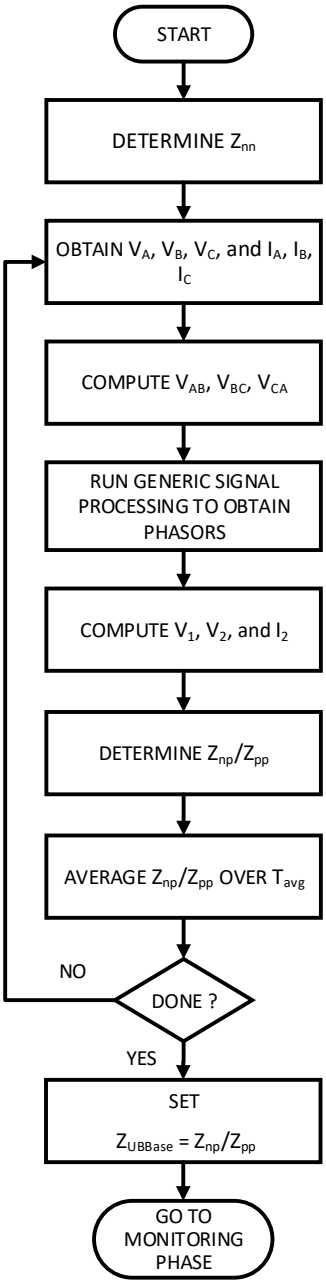

Figure 4.2: Flowchart describing the learning phase [33]

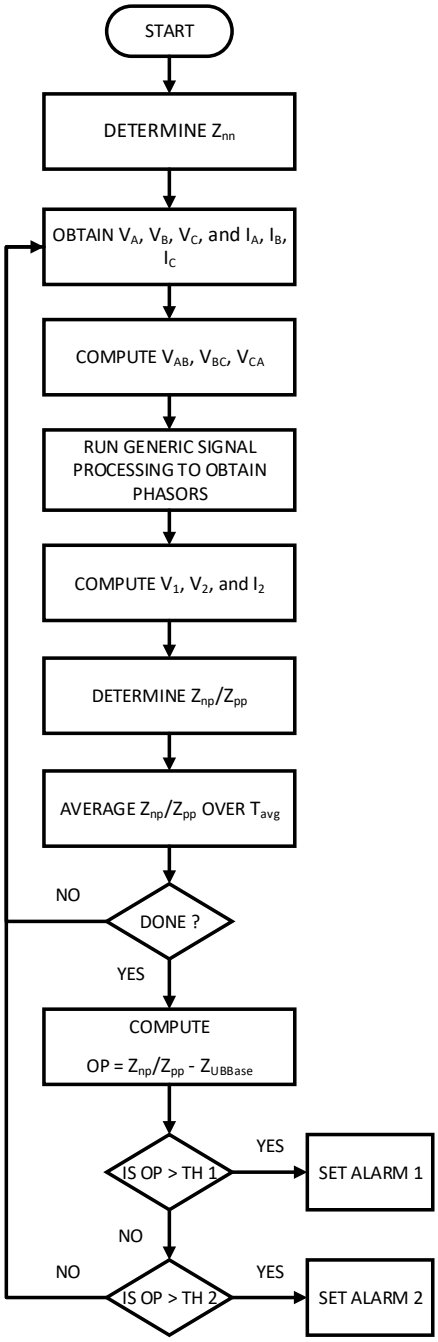

Figure 4.3: Flowchart describing the monitoring phase [33]

- unaltered to system voltage unbalance: any unbalance in the system voltage gives rise to negative sequence component in voltage and subsequently in current. But these negative sequence components are different from the the ones generated due to the fault. The algorithm compensates the effect of any form of unbalance in the system.
- independent of machine ratings: the cross-coupled sequence impedances are machine parameters, therefore machine dependent. But the normalisation of those values with respect to its own base positive sequence impedance makes them independent of machine ratings.
- the algorithm is insensitive to errors in measurement.

4.5. Interconnection between devices

The Omicron Universal relay test set employs multiple analog and digital ports. Figure 4.4 shows the front panel of the test set.

The relay requires 110 V to power up and make a trip contact. The auxiliary DC supply of omicron test set provides this. The Omicron CMC 356 test set has four voltage and six current output channels that can continuously regulate the amplitude, phase and frequency of the signals. All the output channels are protected against over-heating, external transients and overloads. The trip events are recorded by the omicron set up using one of the binary output channels. The experimental test set up for GE multilin relay is as shown in the figure.

The secondary voltage and current signals are fed into the relay by connecting to these voltage and current output ports. The omicron test set has two current outputs that are generally used for differential protection. However, in this case, only one of the current output ports is required. Therefore, the two sets of output ports are shorted manually.

The wiring drawing representing the connections between the relay and the Omicron test set up is shown below:

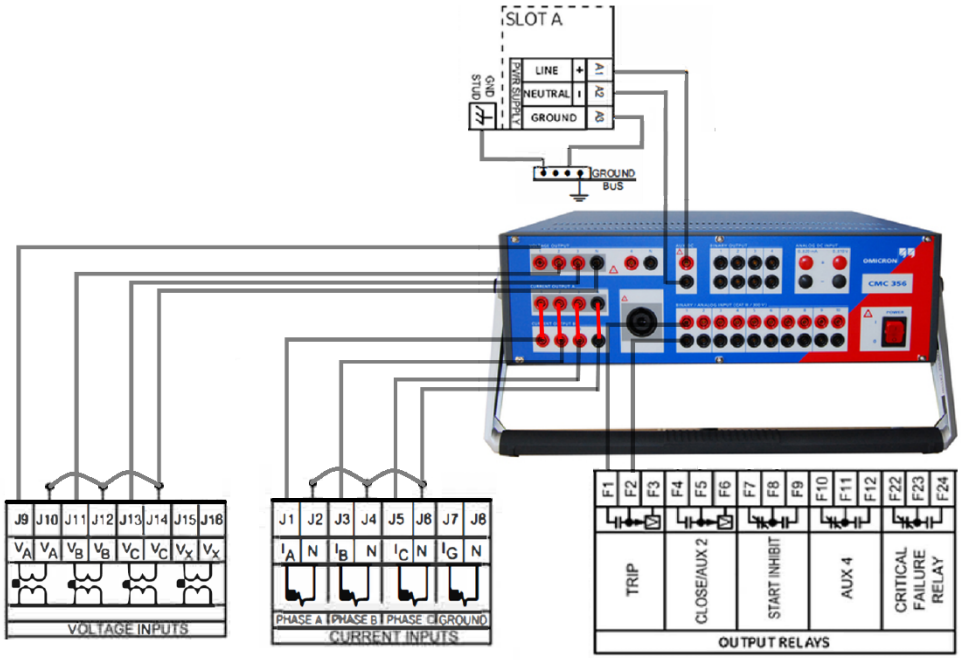

Figure 4.4: Connection drawing between 869 Relay and Omicron test set.

5

Testing of the Relay

The crucial functions of protection relay requires confidence in its operation. The reliability of the relay can be assured by performing tests during its commissioning and scheduled maintenance. Along with a reliability check, regular testing can ensure correct operation of the protection relay during a fault condition. With ageing of the machines, regular testings can also help in optimisation of relay settings to synchronise the protection.

Testing of numerical relays can be done in two ways [34]:

- Primary Injection Testing: These tests involve a complete working circuit: a current transformer, relay, trip alarm and all wiring. These type of testing is generally performed during the commissioning of the relay or protective device.
- Secondary Injection Testing: The purpose of this type of testing is similar to primary injection testing. However, these use a relay test set that can simulate various levels of voltage and current to verify proper relay response as per setting. These type of testing can be performed in a laboratory environment.

The drawback of a primary injection testing is that the test up is expensive and the process is time consuming. Application of faults in the system will affect the remaining network. Therefore, the secondary injection testing type is used here. The testing of the Multilin 869 Relay is done using Omicron CMC 356.

5.1. Procedure of Testing

The output waveforms of EMTP-ATP simulations are saved in ".CFG" or COMTRADE format. COMTRADE stands for **Com**mon format for **Tra**nsient **D**ata **E**xchange.

The ".CFG" file stores sampled data relevant to transients or power system disturbances. With Omicron CMC, ".CFG" files are compatible. Therefore, the output files are directly saved in this format. The .CFG files store the signal names, units, maximum and minimum values of all the signals, number of samples and time of simulation. The ".DAT" file stores all the data sampled at 10^{-4} Hz.

The .CFG files are then uploaded to Advanced transplay module of Omicron and can be tested directly after all the connections between Omicron and the relay module is secured. For testing purpose, the motor start-up is ignored and only steady state and fault condition is considered.

5.2. Test Cases

To determine the sensitivity of the relay with respect to detection of stator inter-turn faults, different test cases are defined by varying the fault resistance and fault severity. The defined test cases are tabulated in the Table 5.1.

Table 5.1: Test cases for the testing of relay

Case No.	R_f (Ω)	μ_{sh}
1	0.1	5
2		10
3		15
4	0.2	5
5		10
6		15
7	0.5	5
8		10
9		15
10	1	5
11		10
12		15
13	2	5
14		10
15		15
16	5	5
17		10
18		15
19	10	5
20		10
21		15

For the function of stator inter-turn fault detection, the default settings of the relay are as tabulated in Table 5.2:

Table 5.2: Default Settings for Stator inter-turn fault Detection

Item Name	Default	Unit	Setting Range
Function	Disabled	-	-
Neg Seq Imp Autoset	Auto	-	Manual, Auto
Neg Seq Impedance	10	Ω	0.10 - 100.00
Pickup Stage 1	0.100	-	0.001 - 10.000
Pickup Delay Stage 1	0.00	s	0.00 - 600.00
Pickup Stage 2	0.600	-	0.001 - 10.000
Pickup Delay Stage 2	0.00	s	0.00 - 600.00
Dropout delay	0.00	s	0.00 - 600.00
Learn turn fault Data	No	-	Yes, No
Block	Off	-	Off, Any FlexLogic
Relay	Do not operate		
Events	Enabled	-	Enabled, Disabled
Target	Latched	-	Self-reset, Latched, Disabled

For the defined test cases, the magnitude of negative sequence component of the input current under fault condition and the resulting operating quantity are tabulated in Table 5.3.

Based on the default threshold of pick up stage 1, the following Table 5.4 tabulates the results.

When the test cases was tested with the recommended settings, the results were unsatisfactory, Therefore, the settings had to be adjusted. The adjustments done in the settings are explained in the following section.

Table 5.3: Operating Point and Negative sequence Component for the defined test cases

Case #	R_f (Ω)	μ_{sh}	OP	I_2 (A)
1	0.1	5	9.50E-03	23.633
2		10	0.05110	64.063
3		15	0.10510	112.11
4	0.2	5	4.80E-03	14.844
5		10	0.03740	48.241
6		15	0.08040	89.648
7	0.5	5	8.70E-03	7.0312
8		10	0.01230	25
9		15	0.02730	53.126
10	1	5	0.01390	3.7109
11		10	5.40E-03	13.672
12		15	0.01630	29.688
13	2	5	0.0025	1,938
14		10	0.0047	7.2269
15		15	0.0075	16.406
16	5	5	0.0002	-
17		10	0.01270	2.9298
18		15	0.01290	6.8362
19	10	5	0	-
20		10	0	-
21		15	0.01450	3.1249

Table 5.4: Test results of the defined test cases with default settings.

Case #	R_f (Ω)	μ_{sh}	Trip
1	0.1	5	No
2		10	No
3		15	Yes
4	0.2	5	No
5		10	No
6		15	No
7	0.5	5	No
8		10	No
9		15	No
10	1	5	No
11		10	No
12		15	No
13	2	5	No
14		10	No
15		15	No
16	5	5	No
17		10	No
18		15	No
19	10	5	No
20		10	No
21		15	No

5.3. Optimisation of Settings in the relay

Based on the defined test cases, to obtain the best possible results, the default settings in the relay are modified. The modified settings are as listed in Table 5.5.

Table 5.5: Modified Settings for Stator inter-turn fault Detection

Item Name	Default	Modified	Unit
Function	Disabled	Enabled	-
Neg Seq Imp Autoset	Auto	Auto	-
Neg Seq Impedance	10	10	Ω
Pickup Stage 1	0.100	0.01	-
Pickup Delay Stage 1	0.00	0.00	s
Pickup Stage 2	0.600	0.600	-
Pickup Delay Stage 2	0.00	0.00	s
Dropout delay	0.00	0.00	s
Learn turn fault Data	No	Yes	-
Block	Off	Off	-
Relay	Do not operate		-
Events	Enabled	Enabled	-
Target	Latched	Latched	-

After the settings were optimised, the tests were performed again. The resulting outcomes are tabulated in Table 5.6.

The relay software records and determines various parameters from the input waveforms. Some of these parameters are plotted in the software as shown in the following Figure 5.1 and Figure 5.2.

The relay records the input current and voltage signals and determines the operating quantity. The increase in negative sequence component and a subsequent decrease in the positive sequence component of the input currents can be observed in the plots. The relay also records the motor status and the trip signal, in case of a trip.

Table 5.6: Test results of the defined test cases with optimised settings.

Case #	R_f (Ω)	μ_{sh}	Trip
1	0.1	5	Yes
2		10	Yes
3		15	Yes
4	0.2	5	Yes
5		10	Yes
6		15	Yes
7	0.5	5	Yes
8		10	Yes
9		15	Yes
10	1	5	Yes
11		10	Yes
12		15	Yes
13	2	5	No
14		10	Yes
15		15	Yes
16	5	5	No
17		10	Yes
18		15	Yes
19	10	5	No
20		10	No
21		15	Yes

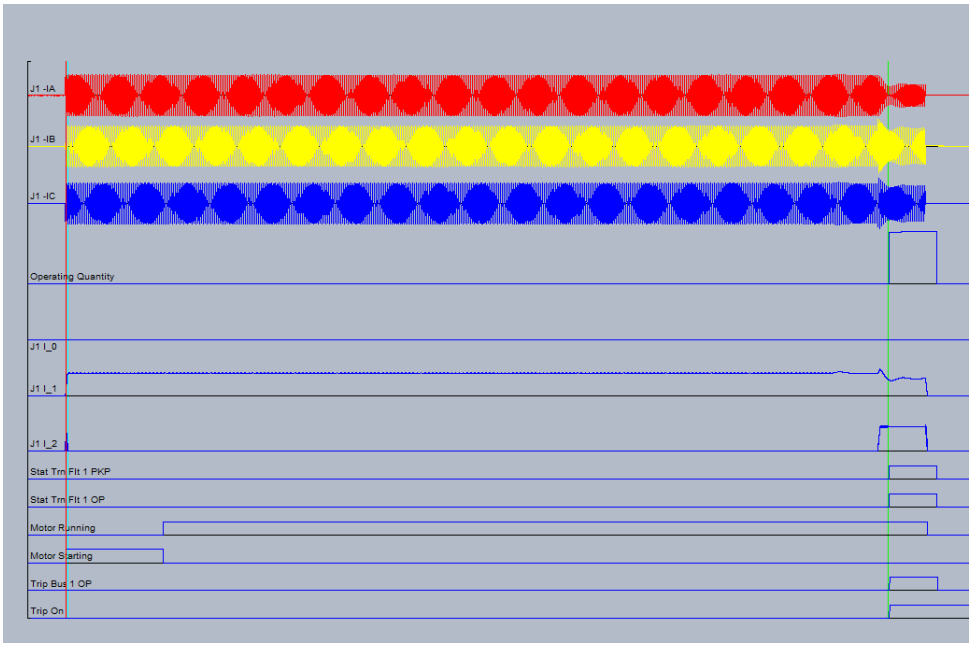

Figure 5.1: Recorded signals during a trip (Case #3)

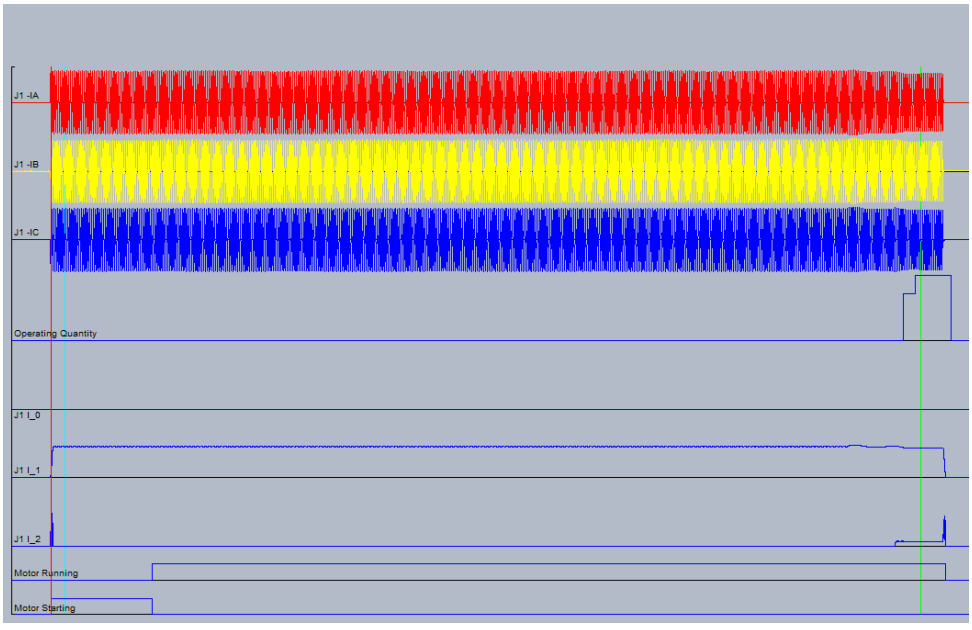

Figure 5.2: Recorded signals during a no trip (Case #13)

5.4. Dead zone of the Relay

The dead zone of a relay is defined as the conditions where the relay fails to detect a fault. In this case, the magnitude of fault is a function of fault severity and fault resistance. To determine the dead zone of the relay, tests are conducted at extremely low fault severities for reasonable fault resistances. From the Table 5.6, it can be observed that the relay detects faults with severity as low as 5% for fault resistances upto 1 Ω. Thus, lower fault severities such as 3% and 4% are considered for fault resistances of 0.5 Ω and 1 Ω to determine the dead zone of this relay. The following tabulates the results.

Table 5.7: Test cases to determine dead zone

Case #	R_f (Ω)	μ_{sh}	Trip	OP	I_2 (A)
1	0.5	3	No	0	-
2		4	Yes	0.01270	4.2968
3	1	3	no	0	-
4		4	Yes	0.01390	2.3442

5.5. Observations

- It can be observed that with increasing fault resistance, the amplitude of fault current is reduced resulting in lower amplitude of negative sequence component. To detect these lower levels of fault, the relay settings are re-optimised. The pick-up stage is reduced to 0.003 from 0.01. Even with the lowest pick up setting, there are cases where the relay does not detect the fault. This is because, the fault current in these cases is too low to produce significant negative sequence component that can be picked up by the relay. The enhanced sensitivity of the relay helps detect the fault at an early stage. This increases the reliability of the system.

- From Table 5.6 and Table 5.7, the lowest fault severity for which the relay trips is 5%. Thus, for a minimum of 0.5 Ω fault resistance, the relay does not detect faults with severities lower than 4% which can be defined as the dead zone of this relay.

- The magnitude of fault current resulting from a stator inter-turn fault is not significant enough to affect the terminal voltage. Therefore, no voltage dip is observed during the fault.

- The algorithm used in the relay was tested on limited set of low powered motors. However, for medium powered induction motors, the value of

the operating point may increase when connected to a unbalanced voltage supply. Therefore, the relay has a wide range of settings.

- The learning of Z_{UBbase} also impacts wide range of settings. This impedance can only be learnt either during the commissioning or the installation of a recently repaired motor. However, in existing installations, the determination of Z_{UBbase} is not possible. Therefore, the relay can consider it to be zero and Z_{np}/Z_{pp} will have a higher value to accommodate the inherent asymmetry of the machine.
- Few other factors affecting the wide range of settings are motor ratings, unbalance from the system, inherent asymmetries of the motor, fault dynamics affecting the negative sequence impedance of the motor.

6

Conclusion

The conventional protection system in use, fails to detect stator inter-turn faults at an early stage. Without early detection, the fault further aggravates into drastic faults such as phase faults. Therefore, a timely detection of such faults becomes a key point of focus. In this thesis, research on stator inter-turn faults and relays protecting against it was conducted.

- **Chapter 1** gave an introduction to the objectives and motivation of the thesis. It described the problem in focus and the scope of work.

- **Chapter 2** described the working principle of an induction machine, its voltage equations and different methods to model it. An introduction to transformation theory and its necessity in modelling rotary machines was discussed. This thesis employed Clarke's transformation to reduce the computational complexity in the model by transforming the three phase quantities to two phase quantities. The induction machine was modelled using the dynamic voltage and torque equations based on these transformed quantities. The latter part of this chapter explained the choice of platform (EMTP-ATP) for modelling and simulation of the machine along with the fault. A validation model was built with default elements to verify the developed model.

- **Chapter 3** explained the typical causes and consequences of stator inter-turn faults in an induction motor. Existing methods to detect such faults were presented. Thereafter, modelling of stator inter-turn fault in the induction motor was described.

- **Chapter 4** gave insight to the principles of motor protection, protection relays and their necessity. The GE Multilin 869 motor protection relay used in this thesis was introduced. The working algorithm used in the relay for detection of a stator inter-turn fault, the parameters used by the relay, and the interconnection with secondary testing kit were also discussed.

- **Chapter 5** explained the testing procedure of the relay and listed out the test cases generated for the stated problem. Based on the finalised test cases, the optimisation of relay settings were explained. Furthermore, this chapter also recorded the dead zone of the relay beyond which the relay cannot detect the fault.

This thesis intended to answer the research questions asked at the beginning of this thesis.

1. **How can an induction machine be modelled accurately to detect stator inter-turn fault?**

   The dynamic modelling of stator inter-turn fault in an induction motor was developed in MODELS environment of EMTP's ATPDraw. This thesis employed Clarke's transformation to reduce the computational complexity in the model by transforming the three phase quantities to two phase quantities. The non-idealities involved in the machine and fault modelling were averted by considering different assumptions. For example, assumptions considered for the progression of fault and fault resistances do not have substantial amount of research. However, due diligence has been done by considering industry data in this area.

2. **How can the fault current resulting from a stator inter-turn fault be detected considering its low magnitude?**

   In this thesis, a medium power induction motor used in a chemical industry was considered. A stator inter-turn fault with varying severities were introduced during the normal operation of this machine and the resulting currents were analysed. As expected, the magnitude of terminal currents did not have much variation after the occurrence of the fault. This is due to the circulatory nature of the fault current. These low magnitude fault current create unbalances in the terminal current that can be used to detect an inter-turn fault.

3. **What is the principle of stator inter-turn fault detection in the chosen protection relay?**

Here, for detection, GE's Multilin 869 motor protection relay is considered. This relay uses sequence cross-coupled impedance for advanced detection of stator inter-turn faults. In an ideal balanced situation, the cross-coupled sequence impedances are zero implying that the positive and negative sequence components of the machine are decoupled. However, in case of a fault, these impedances have small values.These values are used to detect the presence of a stator inter-turn fault.

4. **What are the suitable settings in the chosen protection relay to detect the least severe inter-turn fault without causing any false trips?**

   For the medium power motor in focus, the dead zone of the relay was determined. Based on this dead zone settings were changed from their default values to ensure reliable detection of stator inter-turn faults.

6.1. Discussion

After extensive research, a few discussion point are are listed below:

1. The transformed dynamic model of the induction motor is derived based on the power-invariant Clarke's transformation. The model developed in [35] was taken as a reference. However, discrepancies in the performance characteristics were observed. These were resolved and the machine model was validated with the universal motor model in EMTP-ATP.

2. The detection of a stator inter-turn fault is a monitoring condition rather than a protection function in GE Multilin 869 motor protection relay. Therefore, in case of occurrence of the fault, the relay sends an alarm signal and not a trip signal.

3. When the terminal currents transition from motor start-up to steady state, momentary unbalance occurs. These type of temporary unbalance can be seen during phenomena such as power dips or transfer operations. They give rise to negative sequence components that gets picked up by the Multilin 869 relay. Therefore, the current output waveforms considered for testing does not include motor start-up.

4. The range of settings provided in the relay are broad. The pick up quantity varies from 0.001 to 10.000. This makes the relay highly sensitive. For medium power induction motors, the relay settings for detection of inter-turn fault are to be considered very close to the lower limit. This might result in false alarms.

5. The developed model does not include saturation of the current transformers as low fault currents of such magnitudes are not expected to saturate the transformer.

6. Industries employ vibration monitoring schemes to detect any variations in the speed of the rotor. But the reduced oscillations due to high inertia of the induction motor are not detected by these systems. Therefore, the detection scheme employed by GE Multilin protection relay is required.

6.2. Enhancements proposed by GE

Based on the work done in the thesis, GE has proposed the following enhancements to the relay:

1. The 'Data Quality Check' feature is to be added in the next release. This will help resolve false tripping occurring due to system input. This feature will possibly check temporary power variations, unbalance introduced by the system, frequency variation, and other possible asymmetries.

2. The wide range of settings is to be changed to lower levels assuming proper learning of Z_{UBBase} and Z_{nn}. This can be implemented only after the 'Data Quality Check' feature is included in the relay.

6.3. Future work

This thesis presented a comprehensive method of detecting stator inter-turn faults in induction motors. However, the model designed and the algorithm used for detection have their own drawbacks. Therefore, considerable changes can be inculcated in order to achieve refined results. A few recommendations are presented below based on the work presented.

1. Currently the designed model only considers the effect of stator inter-turn faults on the given network. To further improve the reliability of the network, the model can be made voltage dependent and effect of operations such as power-dips, automatic transfer switching can be observed.

2. An interactive model can be developed that can replicate the progression of an inter-turn fault into a phase-to-ground fault.

3. Algorithms can be included to predict the tripping of relay based on the relay settings.

4. In this thesis, the accuracy of potential core transformer is not considered. The effect of this accuracy on the highly sensitive algorithm can be explored.

Bibliography

[1] P. Albrecht, J. Appiarius, R. McCoy, E. Owen, and D. Sharma, "Assessment of the reliability of motors in utility applications-updated," *IEEE Transactions on Energy conversion*, no. 1, pp. 39–46, 1986.

[2] M. Drif and A. J. M. Cardoso, "Stator fault diagnostics in squirrel cage three-phase induction motor drives using the instantaneous active and reactive power signature analyses," *IEEE Transactions on Industrial Informatics*, vol. 10, no. 2, pp. 1348–1360, 2014.

[3] L. Xiao, H. Sun, F. Gao, S. Hou, and L. Li, "A new diagnostic method for winding short-circuit fault for srm based on symmetrical component analysis," *Chinese Journal of Electrical Engineering*, vol. 4, no. 1, pp. 74–82, 2018.

[4] L. Maraaba, Z. Al-Hamouz, and M. Abido, "An efficient stator inter-turn fault diagnosis tool for induction motors," *Energies*, vol. 11, no. 3, p. 653, 2018.

[5] S. Williamson and K. Mirzoian, "Analysis of cage induction motors with stator winding faults," *IEEE transactions on power apparatus and systems*, no. 7, pp. 1838–1842, 1985.

[6] G. Kliman, W. Premerlani, R. Koegl, and D. Hoeweler, "A new approach to on-line turn fault detection in ac motors," in *IAS'96. Conference Record of the 1996 IEEE Industry Applications Conference Thirty-First IAS Annual Meeting*, IEEE, vol. 1, 1996, pp. 687–693.

[7] X. Luo, Y. Liao, H. A. Toliyat, A. El-Antably, and T. A. Lipo, "Multiple coupled circuit modeling of induction machines," *IEEE Transactions on industry applications*, vol. 31, no. 2, pp. 311–318, 1995.

[8] P. C. Krause, O. Wasynczuk, S. D. Sudhoff, and S. Pekarek, *Analysis of electric machinery and drive systems*. Wiley Online Library, 2002, vol. 2.

[9] L. Dubé, "Users guide to models in atp," *Neskowin OR*, 1996.

[10] L. Dubé, "How to use models-based user-defined network components in atp," in *EUROPEAN EMTP USERS GROUP MEETING*, 1996, pp. 10–12.

[11] "EMTP-ATP beginners training," 2020, ATPDRAW 2020.

[12] H. W. Penrose, "Test methods for determining the impact of motor condition on motor efficiency and reliability," *ALL-TEST Pro, LLC*, 2007.

[13] S. Grubic, J. M. Aller, B. Lu, and T. G. Habetler, "A survey on testing and monitoring methods for stator insulation systems of low-voltage induction machines focusing on turn insulation problems," *IEEE Transactions on Industrial Electronics*, vol. 55, no. 12, pp. 4127–4136, 2008.

[14] A. Strandt, "Characterization of stator winding short-circuit faults in interior permanent-magnet motor-drive systems," 2013.

[15] A. Berzoy, A. Mohamed, and O. Mohammed, "Stator winding inter-turn fault in induction machines: Complex-vector transient and steady-state modelling," in *2017 IEEE International Electric Machines and Drives Conference (IEMDC)*, IEEE, 2017, pp. 1–7.

[16] P. Chen, Y. Xie, and S. Hu, "The effect of stator inter-turn short circuit faults on electromagnetic performances of induction motors," in *2019 22nd International Conference on Electrical Machines and Systems (ICEMS)*, IEEE, 2019, pp. 1–5.

[17] R. M. Tallam, S. B. Lee, G. C. Stone, G. B. Kliman, J. Yoo, T. G. Habetler, and R. G. Harley, "A survey of methods for detection of stator-related faults in induction machines," *IEEE Transactions on Industry Applications*, vol. 43, no. 4, pp. 920–933, 2007.

[18] M. Eftekhari, M. Moallem, S. Sadri, and A. Shojaei, "Review of induction motor testing and monitoring methods for inter-turn stator winding faults," in *2013 21st Iranian Conference on Electrical Engineering (ICEE)*, IEEE, 2013, pp. 1–6.

[19] Y. B. Koca and A. Ünsal, "A review on detection and monitoring of stator faults of induction motors," *International Journal of Innovative Research in Science, Engineering and Technology (IJIRSET)*, vol. 6, no. 10, 2017.

[20] A. Glowacz and Z. Glowacz, "Diagnostics of stator faults of the single-phase induction motor using thermal images, moasos and selected classifiers," *Measurement*, vol. 93, pp. 86–93, 2016.

[21] P. A. Delgado-Arredondo, D. Morinigo-Sotelo, R. A. Osornio-Rios, J. G. Avina-Cervantes, H. Rostro-Gonzalez, and R. de Jesus Romero-Troncoso, "Methodology for fault detection in induction motors via sound and vibration signals," *Mechanical Systems and Signal Processing*, vol. 83, pp. 568–589, 2017.

[22] V. Hegde and G. Maruthi, "Experimental investigation on detection of air gap eccentricity in induction motors by current and vibration signature analysis using non-invasive sensors," *Energy Procedia*, vol. 14, pp. 1047–1052, 2012.

[23] P. Lamim Filho, R. Pederiva, and J. Brito, "Detection of stator winding faults in induction machines using flux and vibration analysis," *Mechanical Systems and Signal Processing*, vol. 42, no. 1-2, pp. 377–387, 2014.

[24] A. Siddique, G. Yadava, and B. Singh, "A review of stator fault monitoring techniques of induction motors," *IEEE transactions on energy conversion*, vol. 20, no. 1, pp. 106–114, 2005.

[25] S.-h. Lee, Y.-q. Wang, and J.-i. Song, "Fourier and wavelet transformations application to fault detection of induction motor with stator current," *Journal of Central South University of Technology*, vol. 17, no. 1, pp. 93–101, 2010.

[26] A. Allal and B. Chetate, "A new and best approach for early detection of rotor and stator faults in induction motors coupled to variable loads," *Frontiers in Energy*, vol. 10, no. 2, pp. 176–191, 2016.

[27] M. Rajagopal, K. Seetharamu, and P. Ashwathnarayana, "Transient thermal analysis of induction motors," *IEEE transactions on energy conversion*, vol. 13, no. 1, pp. 62–69, 1998.

[28] G. C. Stone, E. A. Boulter, I. Culbert, and H. Dhirani, *Electrical insulation for rotating machines: design, evaluation, aging, testing, and repair*. John Wiley & Sons, 2004, vol. 21.

[29] J. Sottile and J. L. Kohler, "An on-line method to detect incipient failure of turn insulation in random-wound motors," *IEEE Transactions on Energy Conversion*, vol. 8, no. 4, pp. 762–768, 1993.

[30] M. Wieczorek and E. Rosołowski, "Modelling of induction motor for simulation of internal faults," in *2010 Modern Electric Power Systems*, IEEE, 2010, pp. 1–6.

[31] R. M. Tallam, T. G. Habetler, and R. G. Harley, "Transient model for induction machines with stator winding turn faults," *IEEE Transactions on Industry Applications*, vol. 38, no. 3, pp. 632–637, 2002.

[32] *869 Stator Inter-turn Fault Detection Application Note*, GET-20059, Multilin 8 Series, GE Grid Solutions, 2018.

[33] P. Ostojic, A. Banerjee, D. C. Patel, W. Basu, and S. Ali, "Advanced motor monitoring and diagnostics," *IEEE Transactions on Industry Applications*, vol. 50, no. 5, pp. 3120–3127, 2014.

[34] *Network Protection & Automation Guide*, E2 Relay Commissioning, Schneider Electric, 2019.

[35] A. T. Saraswathi, "Testing of motor protection for internal faults," 2016.

[36] C. L. Fortescue, “Method of symmetrical co-ordinates applied to the solution of polyphase networks,” *Transactions of the American Institute of Electrical Engineers*, vol. 37, no. 2, pp. 1027–1140, 1918.

[37] R. S. Zhang, “High Performance Power Converter Systems for Nonlinear and Unbalanced Load/Source,” Doctoral Dissertation, Virgina Tech, Nov. 17, 1998. [Online]. Available: http://hdl.handle.net/10919/29314 (visited on 01/05/2021).

Appendices

A

Symmetrical Components

To understand the unbalanced behaviour of three-phase systems, three phase quantities can be transformed into symmetrical components, by using Fortescue transformation [36]. This transformation makes it easier to analyse the unbalanced systems. It also has physical interpretation associated with it [37]. In a three-phase network, the phase-currents I_A, I_B and I_C are given as shown below in Equation A.1:

$$\begin{bmatrix} I_A \\ I_B \\ I_C \end{bmatrix} = \begin{bmatrix} \widehat{I_A} \sin\left(\omega t - \phi_A\right) \\ \widehat{I_B} \sin\left(\omega t - \phi_B\right) \\ \widehat{I_C} \sin\left(\omega t - \phi_C\right) \end{bmatrix} \tag{A.1}$$

where ω is the angular frequency of the sinusoidal waveform and ϕ_A, ϕ_B and ϕ_C represent the phase-difference with respect to the reference angle ωt.

In a balanced condition, the phasors have the same amplitude and are exactly $2\pi/3$ rads apart. Thus, the system can be represented and analysed as an equivalent single-phase system and extrapolate it to the three-phase networks.

In unbalanced networks, the analysis becomes complex as the phasors have different magnitudes and phase differences. To simplify this, Fortescue proposed to transform these three-phase unbalanced phasors into Positive, Negative and Zero-Sequence Components [36]. The decomposition results in three-sets of balanced phasors. The transformation of line currents into their respective symmetric components is done as per the transformation in Equation A.2 [36]:

$$\begin{bmatrix} I_0 \\ I_1 \\ I_2 \end{bmatrix} = \frac{1}{3} \begin{bmatrix} 1 & 1 & 1 \\ 1 & a & a^2 \\ 1 & a^2 & a \end{bmatrix} \begin{bmatrix} I_A \\ I_B \\ I_C \end{bmatrix} \tag{A.2}$$

where $a = e^{j2\pi/3}$, and I_1, I_2 and I_0 are the positive, negative and zero-sequence components of the current respectively. Similarly, the inverse transformation is given in Equation A.3:

$$\begin{bmatrix} I_A \\ I_B \\ I_C \end{bmatrix} = \begin{bmatrix} 1 & 1 & 1 \\ 1 & a^2 & a \\ 1 & a & a^2 \end{bmatrix} \begin{bmatrix} I_0 \\ I_1 \\ I_2 \end{bmatrix} \tag{A.3}$$

B

Developed Model of Induction Motor

The dynamic model of a induction motor with stator inter-turn fault developed using EMTP-ATP is presented.

```
1  MODEL IM_new
2
3  DATA
4
5  rs_new              -- Stator resistance
6  lls_new             -- Stator Leakage inductance
7  ls_new              -- Stator inductance
8  rr_new              -- Rotor resistance
9  llr_new             -- Rotor Leakage inductance
10 lr_new              -- Rotor inductance
11 lm_new              -- Magnetizing inductance
12 rf_new              -- Fault Resistance
13 pp_new              -- Number of Pole pairs
14 f_new               -- Rated frequency
15 tl_new              -- Load Torque
16 j_m_new             -- Motor Inertia constant
17 j_ext_new           -- External Inertia constant
18
19 INPUT
20
21 vi_new[1..3]
```

```
22
23 OUTPUT
24
25 i_new[1..3]
26 vp_new[1..3]
27
28 VAR
29
30 vd_new    vq_new    v0_new          -- Stator
      voltages-Transformed quantities
31 vp_new [1..3]                       -- Potential Tx o
      /p
32 ia_new    ib_new    ic_new          -- Stator
      currents-Phase quantities
33 i_new [1..3]                        -- Current Tx o/p
34 iqs_new   ids_new                   -- Stator
      Currents in DQ frame
35 iqr_new   idr_new                   -- Rotor Currents
       in DQ frame
36 ifa_new                             -- fault current
37 mush_new                            -- % of faulty
      turns  (value ranges from 0 to 1)
38 tem_new                             --
      Electromagnetic Torque
39 tac_new                             -- Accelerating
      Torque
40 ws_new                              -- Synchronous
      Speed
41 wr_new                              -- Rotor speed in
       Electrical Radians
42 nr_new                              -- Rotor Speed (
      in RPM)
43 thetar_new                          -- Rotor angle (
      Mechanical Radians)
44 d1_new  d2_new                      -- Rotor Angle (
      Electrical Radians)
45 fluxqs_new    fluxqspr_new          -- Stator 'q'
      axis flux & Derivative
46 fluxds_new    fluxdspr_new          -- Stator 'd'
      axis flux & Derivative
```

```
47 fluxqr_new     fluxqrpr_new          -- Rotor 'q' axis
       flux & Derivative
48 fluxdr_new     fluxdrpr_new          -- Rotor 'd' axis
       flux & Derivative
49 flux0s_new     flux0spr_new          -- Leakage flux &
       Derivative
50 fluxsh_new     fluxshpr_new          -- Flux in the
      fault part & Derivative
51 f1_new                               -- Load factor
52 j_m_new1                             -- Motor Inertia
      constant
53 j_ext_new1                           -- External
      Inertia constant
54
55 HISTORY
56
57 ia_new {DFLT:0}     ib_new {DFLT:0}     ic_new {DFLT
      :0}
58 iqs_new {DFLT:0}    ids_new {DFLT:0}    iqr_new {DFLT
      :0}  idr_new {DFLT:0}
59 ifa_new {DFLT:0}    wr_new {DFLT:0}     INTEGRAL(
      wr_new){DFLT:0}
60 fluxqs_new{DFLT:0}  fluxds_new{DFLT:0}
61 fluxqspr_new{DFLT:0} fluxdspr_new{DFLT:0}
62 fluxqr_new{DFLT:0}   fluxdr_new{DFLT:0}
63 fluxqrpr_new{DFLT:0}  fluxdrpr_new{DFLT:0}
64 flux0s_new{DFLT:0}    flux0spr_new{DFLT:0}   nr_new{
      DFLT:0}
65 fluxsh_new{DFLT:0}    fluxshpr_new{DFLT:0}
66
67 INIT
68
69 ws_new:=2*pi*50
70 thetar_new:=0       wr_new:=0          tem_new:=0
      ifa_new:=0
71 ia_new:=0           ib_new:=0          ic_new:=0
      tac_new:=0
72 i_new[1..3]:=[0]    vp_new[1..3]:=[0]
73 iqs_new:=0          ids_new:=0         iqr_new:=0
      idr_new:=0
```

```
74  nr_new:=0
75  mush_new:=0
76  j_m_new1:=j_m_new
77  j_ext_new1:=j_ext_new
78
79  ENDINIT
80
81
82  EXEC
83
84  IF t>2 THEN
85  j_ext_new1:=10*j_ext_new
86  j_m_new1:=10*j_m_new
87  ENDIF
88
89  IF t<=2.5 THEN
90  mush_new:=0.00
91  ELSIF t>2.5 AND t<=3 THEN
92  mush_new:=0.03
93  ELSE
94  mush_new:=0.35
95  ENDIF
96
97  -- Calculation of terminal voltages in Park's
       quantities in Power Invariant Form
98  d1_new:=0
99  vd_new:=sqrt(2/3)*(cos(d1_new)*vi_new[1]+cos(d1_new
       -2*pi/3)*vi_new[2]+cos(d1_new+2*pi/3)*vi_new[3])
100 vq_new:=sqrt(2/3)*(-sin(d1_new)*vi_new[1]-sin(d1_new
       -2*pi/3)*vi_new[2]-sin(d1_new+2*pi/3)*vi_new[3])
101 v0_new:=(vi_new[1]+vi_new[2]+vi_new[3])/sqrt(3)
102
103 IF t>0.5 THEN
104
105 COMBINE as FLUX1_new
106
107 --Calculation of Fluxes
108 fluxqspr_new:=SUM(1|vq_new - rs_new|iqs_new + sqrt
       (2/3)*rs_new*mush_new|ifa_new)
109 fluxdspr_new:=SUM(1|vd_new - rs_new|ids_new )
```

```
110 fluxqrpr_new:=SUM(-rr_new|iqr_new + pp_new*wr_new*
       lr_new|idr_new + pp_new*wr_new*lm_new|ids_new)
111 fluxdrpr_new:=SUM(-rr_new|idr_new - pp_new*wr_new*
       lr_new|iqr_new - pp_new*wr_new*lm_new|iqs_new +
       sqrt(2/3)*pp_new*wr_new*mush_new*lm_new|ifa_new)
112
113 --Differential Equation for Fluxes
114 LAPLACE(fluxqs_new/fluxqspr_new):=(1|)/(1|s+0|)
115 LAPLACE(fluxds_new/fluxdspr_new):=(1|)/(1|s+0|)
116 LAPLACE(fluxqr_new/fluxqrpr_new):=(1|)/(1|s+0|)
117 LAPLACE(fluxdr_new/fluxdrpr_new):=(1|)/(1|s+0|)
118
119 ENDCOMBINE
120
121 COMBINE as FLUX2_new
122
123 fluxshpr_new:=SUM(rf_new|ifa_new - mush_new*rs_new|
       iqs_new + mush_new*rs_new|ifa_new)
124 LAPLACE(fluxsh_new/fluxshpr_new):=(1|)/(1|s+0|)
125
126 ENDCOMBINE
127
128 --Calculation of Currents
129 iqs_new:=1/ls_new*(fluxqs_new - lm_new*iqr_new +
       sqrt(2/3)*mush_new*ls_new*ifa_new)
130 ids_new:=1/ls_new*(fluxds_new - lm_new*idr_new)
131 iqr_new:=1/lr_new*(fluxqr_new - lm_new*iqs_new +
       sqrt(2/3)*mush_new*lm_new*ifa_new)
132 idr_new:=1/lr_new*(fluxdr_new - lm_new*ids_new)
133 ifa_new:=(mush_new*ls_new*iqs_new + mush_new*lm_new*
       iqr_new - fluxsh_new)/(mush_new*lls_new + sqrt
       (2/3)*mush_new**2*lm_new)
134
135
136 --Mechanical System
137 IF t<15 THEN f1_new:=0.73 ELSE f1_new:=1 ENDIF
138 tem_new:=(pp_new*lm_new*(idr_new*iqs_new - ids_new*
       iqr_new)-(pp_new*lm_new*mush_new*ifa_new*iqr_new)
       )
```

```
139 tac_new:=(tem_new - ((wr_new/ws_new)**2)*f1_new*
       tl_new)/(j_m_new1+j_ext_new1)
140
141 COMBINE AS MECH_new
142 LAPLACE(wr_new/tac_new):= (1|)/(1|s+0|)
143 thetar_new:=INTEGRAL(wr_new)
144 ENDCOMBINE
145
146 nr_new:= wr_new*(60/2/pi)
147
148 --Inverse Parks' Transformation
149 d2_new:=0
150 ia_new:=sqrt(2/3)*(cos(d2_new)*ids_new       -sin(
       d2_new)*iqs_new       )
151 ib_new:=sqrt(2/3)*(cos(d2_new-2*pi/3)*ids_new-sin(
       d2_new-2*pi/3)*iqs_new)
152 ic_new:=sqrt(2/3)*(cos(d2_new+2*pi/3)*ids_new-sin(
       d2_new+2*pi/3)*iqs_new)
153
154 i_new[1..3]:=[ia_new/200,ib_new/200,ic_new/200]
155 vp_new[1..3]:=[vi_new[1]*110/6300,vi_new
       [2]*110/6300,vi_new[3]*110/6300]
156 ENDIF
157 ENDEXEC
158
159 ENDMODEL
```